


Article

Investigation of Small-Scale Photovoltaic Systems for Optimum Performance under Partial Shading Conditions

Mahmoud A. M. Youssef ^{1,*} , Abdelrahman M. Mohamed ², Yaser A. Khalaf ³  and Yehia S. Mohamed ²¹ Mechanical Engineering Department, Jouf University, Sakaka 72388, Saudi Arabia² Electrical Engineering Department, Minia University, Minia 61519, Egypt; abdo_2024@protonmail.com (A.M.M.); dr.yehia60@yahoo.com (Y.S.M.)³ Electrical Engineering Department, Jouf University, Sakaka 72388, Saudi Arabia; yakhalaf@ju.edu.sa

* Correspondence: myousef@ju.edu.sa

Abstract: Not only are small photovoltaic (PV) systems widely used in poor countries and rural areas where the electrical loads are low but they can also be integrated into the national electricity grid to save electricity costs and reduce CO₂ emissions. Partial shading (PS) is one of the phenomena that leads to a sharp decrease in the performance of PV systems. This study provides a comprehensive performance investigation of small systems (consisting of ten modules or fewer) under all possible shading patterns that result from one shading level (300 W/m² is chosen). The most common configurations are considered for which a performance comparison is presented. Five small systems of different sizes are studied under PS. A new simplifying method is proposed to identify the distinct PS patterns under study. Consequently, the number of cases to be studied is significantly reduced from 1862 to 100 cases only. The study is conducted using the MATLAB/Simulink[®] environment. The simulation results demonstrate the most outperformed configuration in each case of PS pattern and the amount of improvement for each configuration. The configurations include static series-parallel (SP), static total-cross-tied (TCT), dynamic switching between SP and TCT, and TCT-reconfiguration. The study provides PV systems' owners with a set of guidelines to opt for the best configuration of their PV systems. The optimum recommended configuration is TCT reconfiguration, rather than dynamic switching between SP and TCT. The less recommended option, which enjoys simplicity but is still viable, is the static TCT. It outperforms the static SP in most cases of PS patterns.

Keywords: solar photovoltaic; partial shading; maximum power extraction; array interconnection schemes



Citation: Youssef, M.A.M.; Mohamed, A.M.; Khalaf, Y.A.; Mohamed, Y.S. Investigation of Small-Scale Photovoltaic Systems for Optimum Performance under Partial Shading Conditions. *Sustainability* **2022**, *14*, 3681. <https://doi.org/10.3390/su14063681>

Academic Editor: Luis Hernández-Callejo

Received: 7 February 2022

Accepted: 17 March 2022

Published: 21 March 2022

Publisher's Note: MDPI stays neutral with regard to jurisdictional claims in published maps and institutional affiliations.



Copyright: © 2022 by the authors. Licensee MDPI, Basel, Switzerland. This article is an open access article distributed under the terms and conditions of the Creative Commons Attribution (CC BY) license (<https://creativecommons.org/licenses/by/4.0/>).

1. Introduction

1.1. Motivation

Day by day, the demand for electric energy increases, and the need for energy sources to meet these needs increases [1]. Most of the demand for electric power is being met by fossil fuels, which are a finite viable resource, along with the catastrophic environmental problems they cause to the planet. These conditions shed light on renewable energy due to its lasting abundance, environmental friendliness, and low maintenance cost [2,3]. Among the various renewable energy sources, photovoltaic (PV) energy has attracted attention due to its small size and ease of installation in consumption areas, such as rooftops, over-lighting poles, and others. Consequently, it leads to saving energy loss through transmission wires from generation areas to consumption areas. By 2050, it is expected that renewable energy will contribute to 79% of the total energy demand in the world, and PV will be the largest contributor among these energies [4].

Residential small-scale PV systems are currently widely used, and many solutions have been presented to integrate the PV systems in homes. It may be a stand-alone system or with the integration with utility [5,6]. Many advantages have been achieved from the renewable distribution generation as saving the losses of the transmission lines and improving the network frequency [7,8].

However, the PV technology still faces many challenges at the present time, which needs more research, including the problem of low energy generated due to environmental conditions [9]. Usually, there are several connections in series and parallel of the PV modules to obtain the required values of voltage and current [10]. Under normal conditions, sunlight is uniformly distributed over the PV modules, and the characteristic power-voltage curve has a single maximum power point at which the highest power can be extracted [11]. However, due to the presence of many causes of shading such as trees and buildings nearby, the accumulation of dust and clouds passing, the PV modules may not receive an equal amount of solar irradiance. Such effect is known as partial shading (PS) [12]. The PS not only causes a decrease in the output power but also may cause the arising of hotspots as a result of the increased mismatch between PV modules. In order to protect the modules from this effect, bypassing diodes are added to bypass the shaded PV cells or modules. However, this addition causes the appearance of several peaks in the characteristic curve, which makes it difficult to use the traditional tracking techniques to extract the maximum power. Various techniques have been addressed in the literature to solve this problem using metaheuristic methods such as genetic algorithm, cuckoo search, particle swarm optimization, ant colony optimization, and teaching-learning-based optimization [13,14]. Nevertheless, almost all of these techniques require more complex calculations and processing to extract the maximum power.

In [15,16], a simple method is proposed to detect partial shading easily in PV systems. It presents a simple and easy-to-implement controller to track the global maximum power point (MPP). It depends on estimating the voltages at the local maximum power points using only two mathematical equations to control the DC/DC converter.

Recently, many researchers in this area focus on improving the performance of the PV systems under the influence of different environmental conditions, including the partial shading phenomenon. Some researchers focus on developing the internal configuration of the modules to increase their ability to face this phenomenon. For example, article [17] investigated the performance of PV modules with different bus bars configurations for cells. It analyzed seven types of poly-Si PV cells and concluded that the five Busbar cells are the most efficient under PS. Article [18] focused on the modeling and functioning of a half-cell PV module under the PS using the MATLAB software package. Unlike others, the authors of [19] inspected how to reduce the PS effect by using the half-cell modules. They concluded that half-cell modules increase the power by 1.48% in the Fill Factor because of the reduction in electrical losses of cell connectors. The module current also is enhanced by about 3%.

In contrast, another team of researchers focuses on the system as a whole and how to deal with the shading of several modules within the system [20,21]. They investigate various systems under the influence of different PS patterns and experience new methods for static and dynamic connection. Dynamic connection means changing the connection form at the moment of shading. The attempts of this team are explained in detail in Section 1.2.

The contribution of this work concludes all the applications of small-scale PV systems (stand-alone and utility-connected systems). The study investigates the performance of small-scale PV systems for optimum performance under partial shading conditions and presents an effective solution for the PV systems' owners with a set of guidelines to opt for the best configuration of their PV systems. The recommendations increase the output energy yield for the PV systems. Also, the study covers all the possible shading patterns, and to achieve that, a new reduction methodology to eliminate the equivalent patterns has been presented.

1.2. Literature Review

To enhance the performance of solar energy under PS conditions, many efforts have been exerted in this regard. The authors of [20] tested various static configurations of the modules inside the array under 20 different PS patterns. A comparison was made to get the

configuration that gives the best performance between static (series, parallel, series-parallel, bridge-linked, and total cross-tied). The study included three systems of different sizes (3×10), (4×5), and (5×5).

In research [21], a (4×4) system was studied under PS conditions to extract the highest possible power using several different connections. The results were tested and verified through practical experiments. The modeling and evaluation of the performance of a system (7×7) under 14 shading patterns were discussed in [22]. The output power, voltage, and current at the maximum power point along with the number of local maximum points were compared. In research [23], a (2×4) system was studied under several shading patterns through MATLAB simulation and experimental verification. The results showed that the total-cross-tied (TCT) method provided the best performance, but the research did not include all possible shading patterns. In [24], six possible configurations for a (5×4) system were tested under PS. TCT was the best one when a column is entirely and unevenly shaded.

Due to the demerits of the static form of the PV configuration, researchers have proposed to make a dynamic change of electrical connections according to the PS situation to give the best performance. In [25], static and dynamic reconfiguration techniques were studied to enhance a PV system's performance. In [26], a (6×4) system was studied under four different levels of solar irradiance and the results were experimentally verified. In [27], a study was carried out on a (6×6) system under three levels of irradiance and a comparison between the TCT technique and magic square technique was introduced.

In [28], the triple-tied configuration was studied and its performance was compared with the other techniques. Authors in [29] studied different reconfiguration techniques and a new scheme was presented to improve the performance of the system. Furthermore, authors in [30] presented a comprehensive study about static, reconfiguration, and meta-heuristic interconnection schemes. TCT, Su-Do-Ku, Dominance square, competence square, and a proposed array configuration were studied in detail in [31]. A new Su-Do-Ku PV configuration is proposed like hyper Su-Do-Ku and compared with the already existing PV array configurations in [32]. Research [33] presented a new socio-inspired PV reconfiguration approach, called democratic political to effectively reduce the mismatching power losses. Three case studies were carried out to verify the proposed technique. On the other side, research [34] focused on large-sized systems such as (16×16) and (25×25). Also, research [35] assessed the shading losses in a large PV power plant with 2.85 MW nominal power and 10,010 modules. It introduced a methodology for the assessment of annual energy loss for the large PV stations.

An improved dynamic array reconfiguration strategy was proposed based on current injection in [36]. In this strategy, the output power output and the multiple peaks in the PV array characteristic curve were also avoided. However, it needed some modifications in the power converters. A dynamic L-shaped reconfiguration was presented in [37], relying on changing each array connection to be in the form of letter L to enhance the amount of power generated from the system. In addition, a new array configuration was presented. Re-allocation of a PV module-fixed electrical connection was introduced in [38] where a new proposed "Shape-do-ku" puzzle was presented and simulated for a (4×4) system.

1.3. Novelty of Work

Most of the past research focused on studying PV systems under the influence of a specific number of shading patterns, but the PS patterns cannot be fully evaluated. Moreover, most of the previous studies focused on large systems, and there are no comprehensive studies on small systems, despite their prevalence in the homes of low-consumption rural areas. In addition, small PV systems can be used in urban houses to partially supply the required electricity and to integrate into the public electricity grid. They can be sometimes used to energize streetlights on highways. On the other side, with the development of manufacturing technology and the use of multilayer boards, the resulting capacity of one module is increasing. That makes the PV systems need a smaller number of PV modules

for the same power generated. However, the loss of electricity resulting from one module as a result of partial shading is more effective.

Our study comes here as a good contributor in this area of research.

1. It provides a comprehensive investigation of the performance of small PV systems (consisting of 10 modules or fewer) rather than for large systems as in most previous studies.
2. PV systems are tested under all possible shading patterns as a result of a single shading level (300 W/m^2) for common wiring configurations rather than for a set number of patterns as in previous studies.
3. To be able to cover all possible PS patterns, a new reduction methodology is proposed to eliminate the equivalent patterns. Consequently, the number of studied patterns is limited to a feasible value as low as 100 cases.
4. The study affords a few recommendations for the proper choice of the PV system configuration, seeking optimum performance under PS conditions.

2. Mathematical Modeling

There are several ways to model a PV cell as a single diode model (SDM), double diode model, and triple diode model. SDM does not provide highly accurate results in large systems due to inherent variations in cell characteristics [24].

However, since the study is concerned with small systems, SDM would be appropriate for both simplicity and a reasonable level of accuracy. SDM PV equivalent circuit is illustrated in Figure 1.

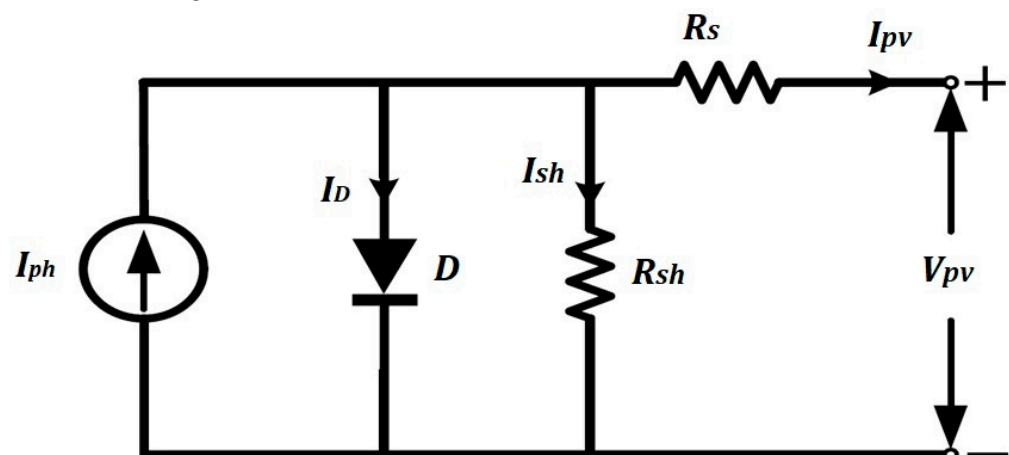


Figure 1. Single diode model PV equivalent circuit.

SDM is also available in Simulink as in Figure 2, which makes it easier to re-study for similar systems with different variables. The current of PV cell is related to the module voltage, thermal voltage, series and parallel resistance, and diode ideality factor as:

$$I_{pv} = I_{ph} - I_0 \left(e^{\frac{V_{pv} + I_{pv} R_s}{a V_t}} - 1 \right) - \frac{V_{pv} + I_{pv} R_s}{R_{sh}} \quad (1)$$

where I_{pv} : output current of the PV cell, I_{ph} : light generated current, I_0 : reverse saturation current, R_s : series resistance, a : diode ideality factor, R_{sh} : shunt resistance, and V_t : thermal voltage of the module which is given as:

$$V_t = \frac{K T N_s}{q} \quad (2)$$

where K : Boltzmann’s constant, T : absolute temperature in Kelvins, q : electron charge, N_S : number of series cells. The generated current is directly related to the amount of irradiance as:

$$I_{ph} = (I_{SC,STC} + K_i(T - T_{STC})) * \frac{G}{G_{STC}} \tag{3}$$

where G : solar irradiance, K_i : temperature coefficient of short circuit current, and T_{STC} : reference temperature at the standard test conditions (STC). The standard test conditions are defined by: $G_{STC} = 1000 \text{ W/m}^2$, air mass ratio = 1.5, and temperature of the module = $25 \text{ }^\circ\text{C}$.

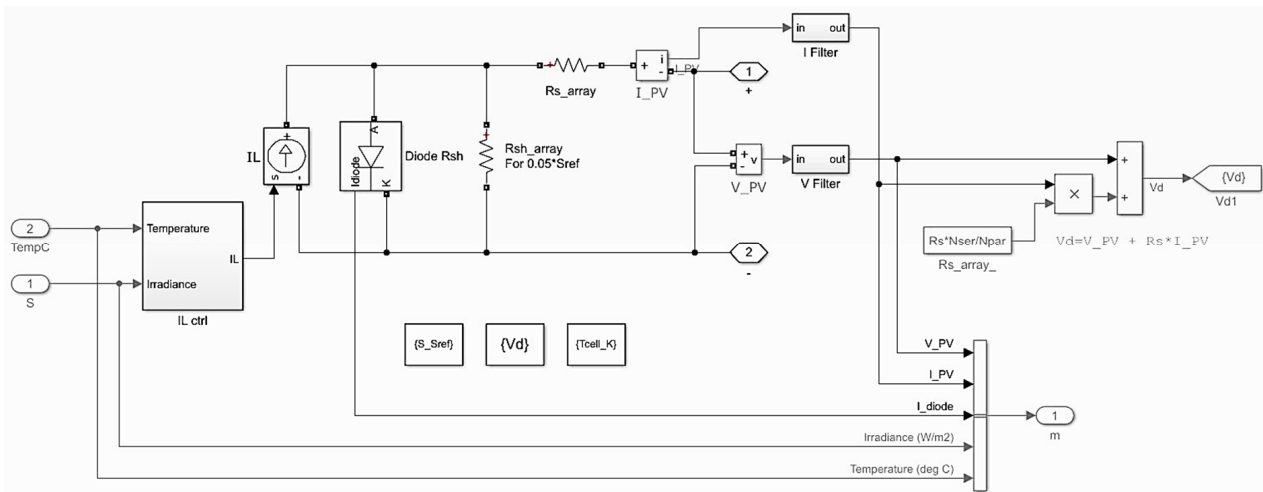


Figure 2. Default MATLAB Simulink model.

Finally, the reverse saturation current can be extracted from open circuit voltage V_{OC} at STC and temperature voltage coefficient K_V as:

$$I_0 = \frac{I_{SC,STC} + K_i(T - T_{STC})}{e^{\frac{V_{pv} + I_{pv}R_s}{aV_t}} - 1} \tag{4}$$

Suntech Power STD275-24-Vd PV module is used where its parameters and data specification are taken from the database of National Renewable Energy Laboratory (NREL) as in Table 1.

Table 1. Electrical characteristics of Suntech Power STD275-24-Vd PV module.

Parameter	Value
Maximum power (W)	275.184
Cells per module N_s	72
Open circuit voltage (V)	44.7
Short circuit current (A)	8.26
Voltage at maximum power point (V)	35.1
Current at maximum power point (A)	7.84
Voltage temperature coefficient (%/ $^\circ\text{C}$)	-0.313
Current temperature coefficient (%/ $^\circ\text{C}$)	0.053995
Diode saturation current I_0 at STC (A)	4.8633×10^{-11}
Diode ideality factor	0.93444
Shunt resistance (Ω)	830.73
Series resistance (Ω)	0.57826
Module efficiency at STC	14.2%
Dimension	$1.956 \text{ m} \times 0.992 \text{ m}$

To validate the model, the simulated results are compared with the practical data (taken from the datasheet [39]) of the Suntech Power STD275-24-Vd PV module. Figure 3a,b represents the I-V and P-V curves for the designed model and datasheet. It is observed that there is an agreement between the model results and the practical data.

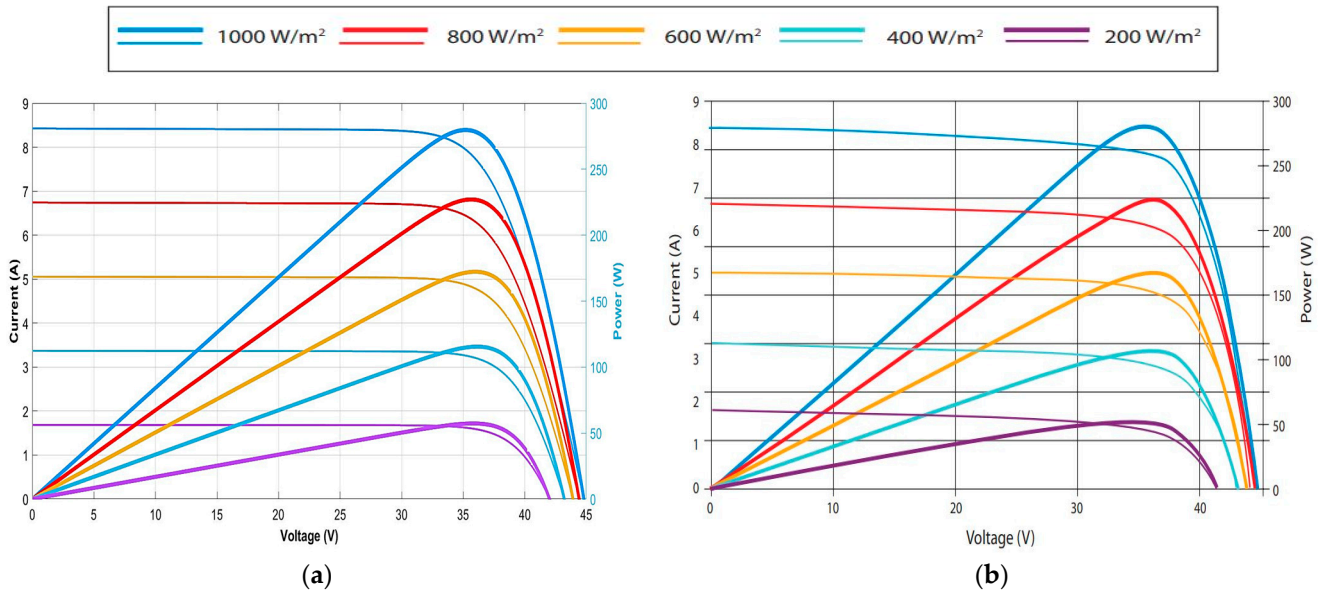


Figure 3. I-V and P-V curves at different radiation levels (a) Simulation results (b) Datasheet curves.

3. System Description

In this study, the focus is on small PV systems, which are identified as systems with 10 modules or fewer. A comprehensive study of these small systems under PS conditions is introduced. Since there are not many possible ways to connect small systems (unlike large systems), it can be considered that they are mainly limited to a small number of common static configurations as (Series, Parallel, series-parallel (SP), and total-cross-tied TCT).

Since the series configuration is characterized by being the least in the number of connecting wires, it has several disadvantages such as: the low value of the current produced under normal conditions, the large value of the voltage on both ends of the system, and the significant decrease in the generated power when PS occurs [14]. In contrast, the parallel configuration is characterized by having one maximum power point under both normal conditions and PS conditions. It also gives the highest power under PS conditions. Nevertheless, it is disadvantaged by the large amount of current passing through the installation and into the inverter or batteries, as well as low output voltage levels [16]. This makes both methods unfavorable options in most cases. Therefore, it can be considered that the comparison is mainly between SP and TCT for static configurations. Also, dynamic switching between SP and TCT is proposed to be investigated in addition to TCT-reconfiguration (in which the shaded module positions are changed according to the PS pattern).

PV systems can be divided into two main types:

- i. Symmetrical dimension systems: symmetrical systems that consist of 10 modules or fewer with equal numbers of rows and columns are mainly configured in two systems (2×2) and (3×3).
- ii. Asymmetrical dimension systems: asymmetrical systems are those in which the number of rows is not equal to the number of columns. Asymmetrical systems that consist of 10 modules or fewer are mainly configured in three systems (2×3), (2×4), and (2×5).

4. Shading Patterns Description

Although the probability of some shading patterns is greater than other patterns, it is difficult to predict the typical shading pattern. Moreover, some shading patterns arise after the installation of the system. What distinguishes this research is the possibility of studying all shadow patterns that may occur in small PV systems resulting from one level of shading. A shading level of 300 W/m^2 is chosen, while the normal condition is a solar irradiance level of 1000 W/m^2 . It is also considered that the module temperature is constant at $25 \text{ }^\circ\text{C}$.

Because of the limited size of the system, all possible shading patterns can be identified and counted as in Table 2. There are 1862 possibilities for the five PV systems. A simplifying method is presented to reduce the number of shading possibilities. In order to avoid repetition, it is sufficient to keep one case in which the shading pattern is similar in both connections' SP and TCT. So, all patterns in which the number of shaded modules in all rows and columns of the first pattern is equal to all rows and columns of the second type are characterized by giving an equal performance in both configurations of SP and TCT.

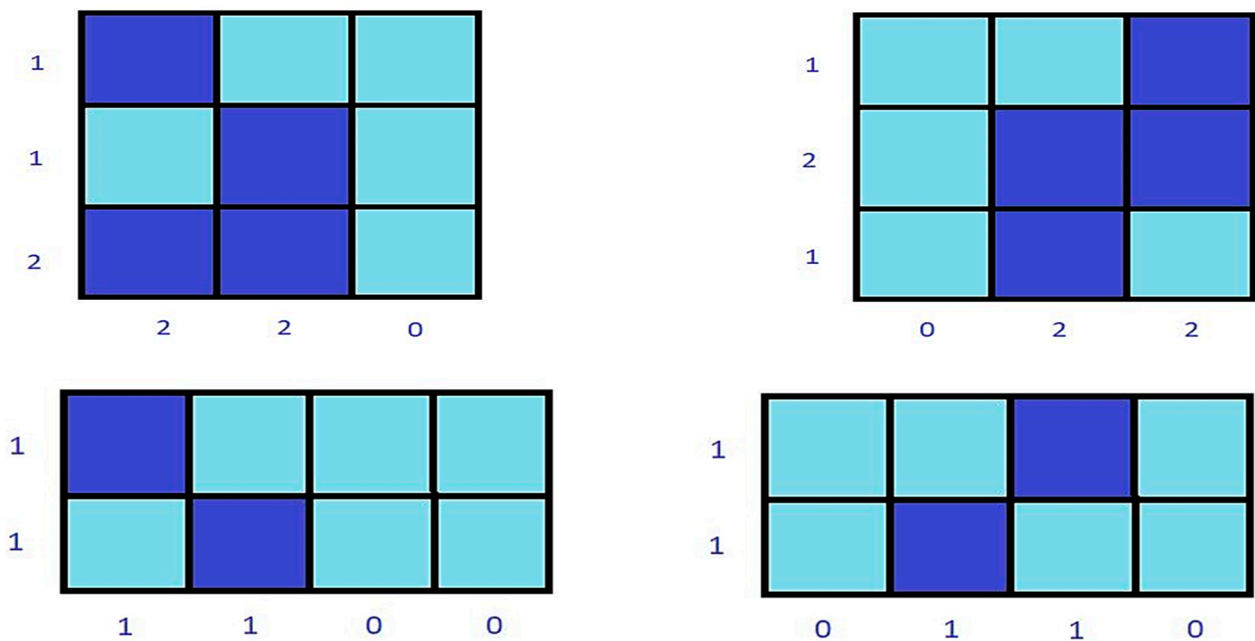


Figure 4. Examples to explain the simplifying method.

Table 2. Number of possible shading patterns before and after applying the simplifying method.

System	Number of PS Patterns	Can Be Simplified to a Repeated Distinguish Patterns Number of
2 × 2	4C1 = 4	1
	4C2 = 6	3
	4C3 = 4	1
	Total = (14)	Total = (5)
2 × 3	6C1 = 6	1
	6C2 = 15	3
	6C3 = 20	3
	6C4 = 15	3
	6C5 = 6	1
	Total = (62)	Total = (11)

Table 2. Cont.

System	Number of PS Patterns	Can Be Simplified to a Repeated Distinguish Patterns Number of
2 × 4	8C1 = 8	1
	8C2 = 28	3
	8C3 = 56	3
	8C4 = 70	6
	8C5 = 56	3
	8C6 = 28	3
	8C7 = 8	1
	Total = (254)	Total = (20)
3 × 3	9C1 = 9	1
	9C2 = 36	3
	9C3 = 84	6
	9C4 = 126	6
	9C5 = 126	6
	9C6 = 84	6
	9C7 = 36	3
	9C8 = 9	1
Total = (510)	Total = (32)	
2 × 5	10C1 = 10	1
	10C2 = 45	3
	10C3 = 120	3
	10C4 = 210	6
	10C5 = 252	6
	10C6 = 210	6
	10C7 = 120	3
	10C8 = 45	3
	10C9 = 10	1
Total = (1022)	Total = (32)	
Five systems	Total = 1862	Total = 100

For example, when studying the system shown in Figure 4, it is noticed that both patterns of PS give the same performance when connected to the two configurations under study. Consequently, it is sufficient to study only one pattern of the two. In other words, swapping a column for another column, or a row for another row does not affect the performance of the system for both SP and TCT.

This limits all possible shading patterns to a limited number for comparison. From Table 2, it is clear that the proposed method reduces the probable cases from 1862 to only 100 cases, which can be conveniently studied.

5. Performance Parameters

To compare different configurations, performance assessment parameters must be determined to choose the best configuration that gives the highest performance. Selected factors are open-circuit voltage V_{OC} , short-circuit current I_{SC} , global maximum power point

voltage V_{GMPP} , global maximum power point current I_{GMPP} , power losses, and the number of local maximum power points.

The mismatching power loss, PL % is given by:

$$\text{Power loss, } PL \% = \frac{P_{MPP} - P_{PSC}}{P_{MPP}} \times 100 \quad (5)$$

where P_{MPP} and P_{PSC} are the maximum power point values without any shading and with PS condition, respectively. As the PL value is less, the performance of the PV system is higher.

The ratio of maximum power output to the input irradiance power is called the efficiency η % and calculated by (7):

$$\text{Efficiency, } \eta \% = \frac{V_{MPP} \times I_{MPP}}{G \times A} \times 100 \quad (6)$$

where G is the solar irradiance and A is the net array area. As the η value is higher, the performance of the PV system is better.

To measure the difference between static SP and TCT a simple equation is used. It is considered that static TCT is better than static SP by (K_T %) defined as:

$$K_T \% = \frac{P_{TCT} - P_{SP}}{P_{TCT}} \times 100 \quad (7)$$

Also, to measure the difference between static TCT and Reconfigurable TCT another simple equation is used. It is considered that reconfigurable TCT is better than static TCT by (K_{RT} %) defined as:

$$K_{RT} \% = \frac{P_{TCT \max} - P_{TCT}}{P_{TCT \max}} \times 100 \quad (8)$$

where $P_{TCT \max}$ is the maximum power for the same number of shaded modules using reconfigurable TCT technique

6. Simulation Results and Discussion

This section evaluates systems' performance and shows the simulation results. The diagram in Figure 5 demonstrates the research methodology. For every PS case, the results are divided according to the number of shaded modules where the highest performance data is bolded if any. The measured parameters are V_{OC} , I_{SC} , V_{GMPP} , I_{GMPP} , P_{GMPP} , PL , efficiency, and the number of local MPPs. The comparison for every case is between static SP, static TCT, the dynamic change between them, and reconfigurable TCT.

The most important performance parameter in this comparative study is the global maximum power of the PV system. For this reason, our discussion is fundamentally based on the output power of the PV system under various shading patterns to evaluate different connectivity configurations. The best connectivity configuration is the one that produces the highest power under specific shading conditions for the same system. Although other performance parameters are of less importance, they are fully reported in the tables of Appendix A for the sake of completeness. In addition, the I-V and P-V characteristic curves of the different systems under study are also included in Appendix A for full characterization of the system.

6.1. Symmetrical Dimension Systems

6.1.1. System 2×2

System 2×2 consists of five possible cases, which can be classified into four sections according to the number of shaded modules. Figure 6 explains the output power for all system 2×2 cases. For one shaded module (case 1), TCT presents a better performance (with 774.6 W output power) than that of SP (726.2 W). The same observation can be applied when all the modules are shaded except one (as in case 5). Reconfigurable TCT cannot

add new information as there are no multiple cases to choose from for the same number of shaded modules.

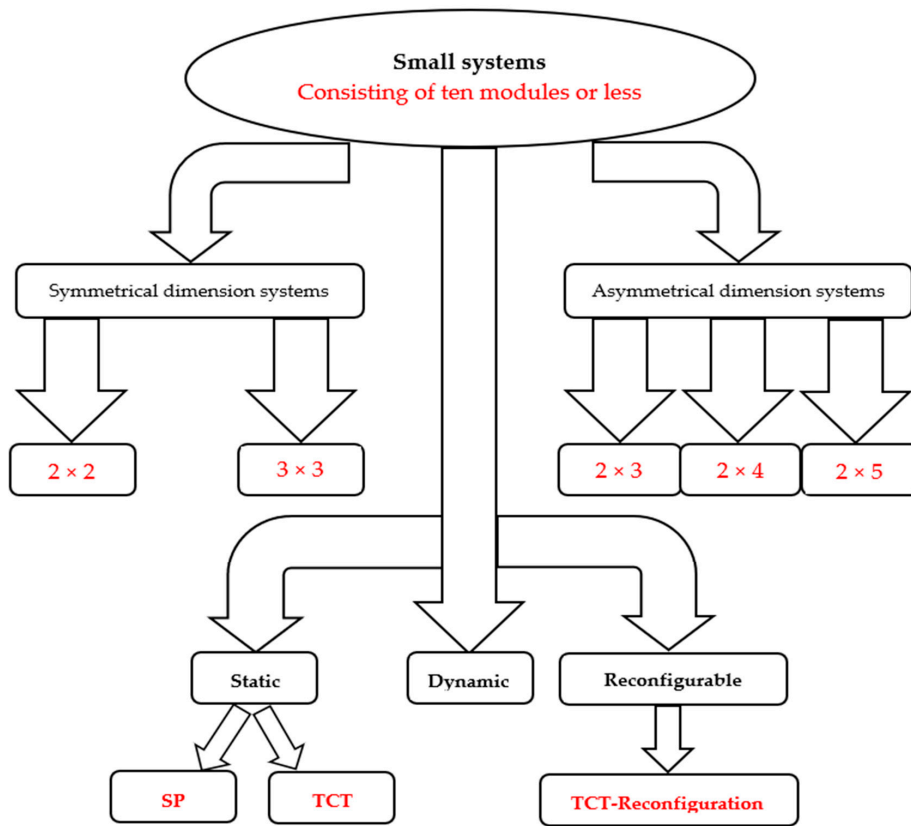


Figure 5. Diagram explaining the research methodology.

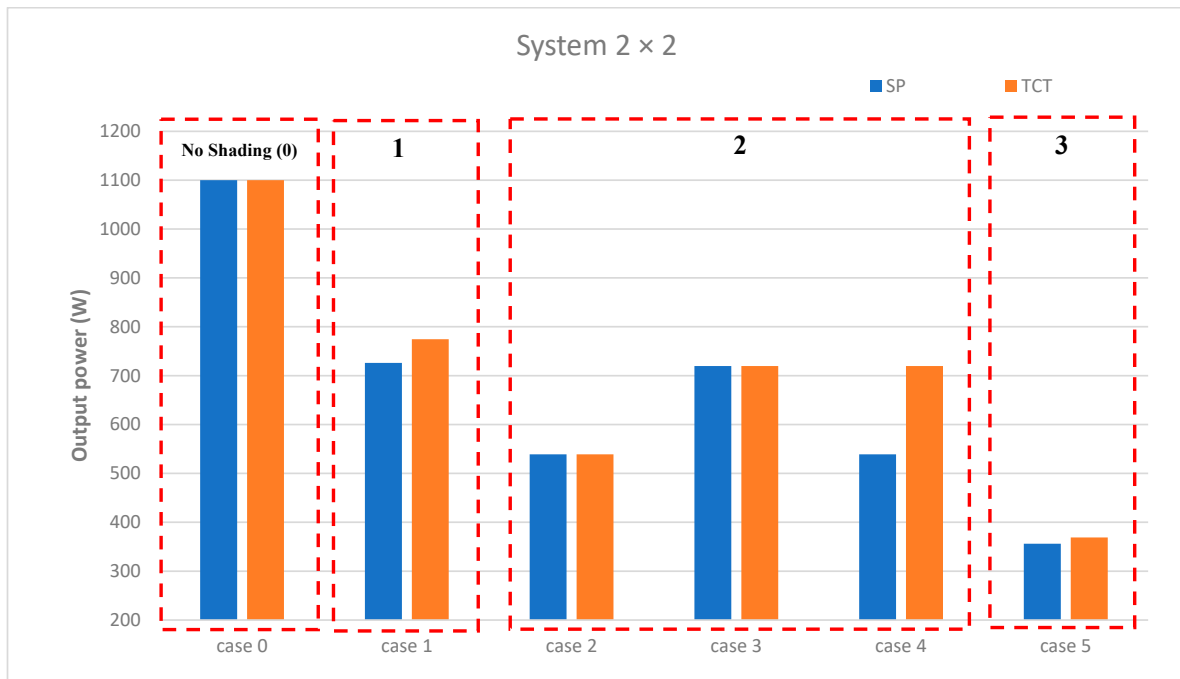


Figure 6. Bar chart of the output power for all 2 × 2 system cases.

However, when two modules are shaded, there are three cases (Case 2, 3, and 4). In case 2, TCT has the same performance as SP (with 539.1 W output). Case 3 also has the

same performance for SP and TCT (with 719.1 W output). In case 4, TCT (with 719.1 W) is better than SP (with 539.1 W). So, it is observed that dynamic change between SP and TCT is useful only for case 4 and cannot improve the performance in either case 2 or case 3. On the other hand, with reconfigurable TCT, the shade pattern can be changed from case 2 to case 3 or 4 with an improvement in output power by 25.09%. That ensures the best performance for two shaded modules.

In the case of static configuration, it is clear that the TCT configuration achieves better results in terms of the amount of power generated in three out of five possible cases, while it is equal to the SP configuration in only two cases. As a result, the dynamic switching between the two configurations does not introduce any advantage.

In the case of TCT-reconfiguration, the amount of improvement in the resulting power is only in one case out of the five cases, with a noticeable increase in the amount of power and a single MPP in the I-V curve. Reconfigurable TCT reduces the number of maximum power points to the least possible value among all cases of TCT. Figure A1 shows the I-V and P-V characteristic curves of the five cases, divided according to the number of shaded modules. The curves indicate the numbers and positions of local maximum power points as well as the position of the global maximum power point. V_{MPP} of TCT in all cases (except case 2) is near to the V_{OC} values. In contrast, with TCT reconfiguration, the V_{MPP} of all cases is kept near to the V_{OC} values. Table A1 presents more details about the simulated results and of the performance parameters for various shading cases.

6.1.2. System 3×3

Practically, system 3×3 is more common than 2×2 . System 3×3 has 32 possible shading cases, which can be divided into eight sections according to the number of shaded modules. The bar chart of the output power for different cases is shown in Figure 7. Again, for one shaded module (case 1), TCT presents a better performance (with 2067 W output power) than SP (1914 W). The same conclusion can be drawn for case 32 with different power levels. Thus, reconfigurable TCT cannot introduce any improvement for the first and last cases. With two shaded modules (case 2, 3, and 4), the results are similar to that of the 2×2 system. TCT reconfigurable ensures the best output power (with 1978 W) where the dynamic change to SP improves case 2 (to 1674 instead of 1634). However, this does not ensure the best performance for the two shaded module cases.

With three shaded modules, there are six possible cases (5 to 10). TCT reconfigurable here has more effective results as it can choose from six different cases. It can change from shade pattern in (case 5, 6, or 7) to give the highest possible power (of 1905 W). The improvement ratios are 14.2%, 22.3%, 22.3% for the three cases, respectively. The same result can be observed at the state of four shaded modules, but with smaller improvement ratios (8.76%, 3.56%, and 3.56% for cases 11, 13, and 14, respectively).

For the rest shading states, symmetry is observed. The states of five, six, seven, and eight shaded modules are similar to four, three, two, and one shaded modules, respectively. This is due to the symmetric dimension of the system.

It can be inferred from Figure 7, that the TCT method is superior in 24 out of 32 possible cases, while it is equal to the SP method in only four cases. Consequently, in the case of static configuration, SP configuration is not preferred, while the dynamic switching between the two configurations improves only four cases by a small percentage in most cases. The location of the same number of shaded modules significantly affects the system performance. For this reason, reconfigurable TCT has a significant effect on the performance. With the TCT reconfiguration technique, the performance is improved in 16 cases, which represents 50% of all the possible cases, and the percentage of power improvement is larger compared to the dynamic method. So, the TCT reconfiguration technique is highly recommended. Five cases (4, 7, 14, 15, and 28) have significantly smaller V_{MPP} in SP than TCT, where only one case (27) has the opposite state. From Figure A2b, it is observed that with TCT reconfiguration, case 3 may be the best replacement for the different shading patterns with a good position of the global MPP. The same observation can be extracted

from Figure A2a–e. The simulated results of different performance parameters are reported in Table A2.

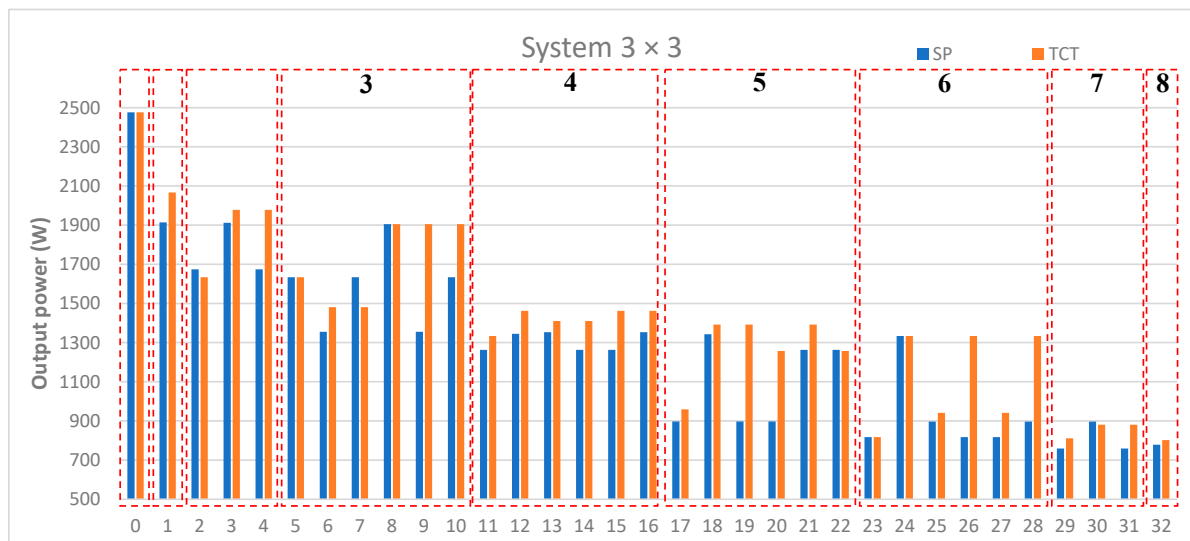


Figure 7. Bar chart of the output power for all 3×3 system cases.

6.2. Asymmetrical Dimension Systems

They comprise the systems in which the number of rows does not equal the number of columns, including systems 2×3 , 2×4 , and 2×5 . Here, 11, 20, and 32 cases are presented for systems 2×3 , 2×4 , and 2×5 , respectively.

6.2.1. System 2×3

The 2×3 system is considered one of the simplest cases of asymmetric systems and is characterized by 11 possible PS cases for one level of shading when comparing between TCT and SP. Figure 8 shows the bar chart of the output power for all system shading cases. When one module is shaded, TCT presents better output power by 5.3% than SP. The same result is found in the case of shading five modules (TCT is 4.9% better than SP). At the state of two shaded modules, TCT is better than SP in case 2 (with output power 6.61% higher) and case 4 (with output power 28.78% higher). However, TCT gives the same performance as SP in case 3. Reconfigurable TCT can change the shading pattern in case 3 to achieve an output power of 1270 W with an improvement ratio of 23.74%. Three and four shaded modules states are similar to the two shaded in the output performance but with a smaller output power owing to the wider shaded area. There is also an exception in case 8 where SP is better than TCT by a smaller ratio (0.5%). However, the optimum performance for four shaded modules can be achieved with reconfigurable TCT as in cases 9 and 10. Thorough simulation results of the performance parameters under various shading conditions can be found in Table A3.

In summary, the TCT method is superior in 7 out of 11 possible cases, while it is equal to the SP method in three cases. SP is outperformed in only one case by a very small percentage. This shows that in the case of static configuration, TCT is highly preferred over the SP configuration. The dynamic switching between the two configurations does not introduce any significant effect. In the case of TCT-reconfiguration, it is noticed that the performance improves in three cases, with a high percentage of power improvement. It is interesting to note that TCT provides higher V_{MPP} values almost in all cases than that of the SP method. The I-V and P-V characteristic curves of the eleven cases are shown in Figure A3, classified according to the number of shaded modules. From every figure (from Figure A3a–e), representing a specific state, the best TCT, which is a used case for the TCT reconfiguration, can be easily extracted along with the position of the MPP location.

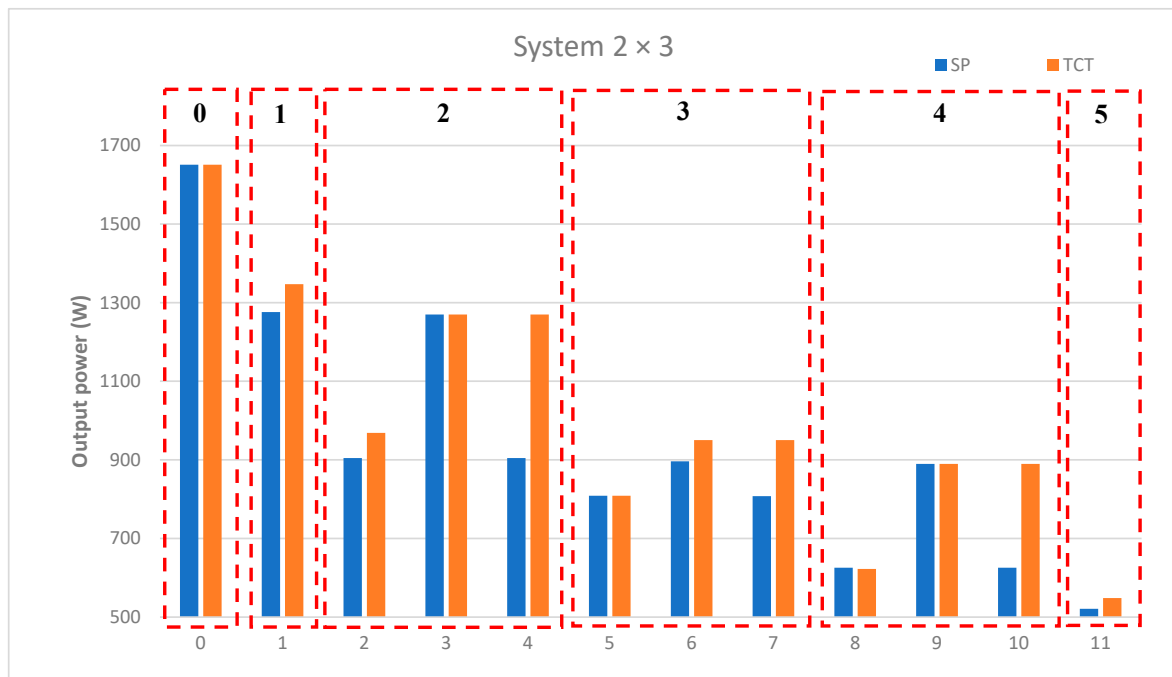


Figure 8. Bar chart of the output power for all 2×3 system cases.

6.2.2. System 2×4

System 2×4 is characterized by 20 possible shading patterns for one shading level when comparing TCT and SP. The simulated output power is demonstrated in Figure 9. One, two, and three shaded modules states are similar in the general performance to those of 2×3 systems with just different output power values. However, four shaded modules states have six possible cases. TCT performance is equal to SP in two cases (8 and 11 with 1078 W) and TCT is better in the rest four cases (with 1146 W for cases 9 and 10 and 1439 W for cases 12 and 13). This gives the reconfigurable TCT the ability to improve four cases to give 1439 W with an improvement ratio of 20.36% (for cases 8 and 11) and 25.1% (for cases 9 and 10). Five, six, and seven shaded modules states are similar in the general performance to three, two, and one shaded modules states, respectively. In addition, more improvement ratios are remarkable when using reconfigurable TCT with 20.73% in case 14 and 30.38% in case 17.

In conclusion, the TCT method is superior in 15 cases, while it is equal to the SP method in four cases only. SP is better in only one case by a slight percentage. It is noticeable here that TCT presents higher V_{MPP} values in seven cases than SP, while the voltage values are almost equal in the rest cases.

Again, in the static configuration, the SP method is not highly preferred when compared to TCT, while the dynamic switching between the two configurations does not add any significant effect. In the case of TCT-reconfiguration, the performance improves in seven cases, with a significant percentage of power improvement. For complete characterization of the performance parameters, one may refer to Table A4. The I-V and P-V characteristic curves of the 20 cases are shown in Figure A4.

6.2.3. System 2×5

System 2×5 has 32 cases and can be classified into nine groups according to the number of shaded modules. Figure 10 explains the output power for all 2×5 system cases. The TCT method is better than SP in 23 cases with a ratio of output power improvement between 4% and 31.36%. In contrast, SP is slightly better in only three cases 16, 20, and 26 with output-power improvement percent of 0.82%, 0.26%, and 0.65%, respectively. For the remaining six cases, SP gives the same performance as TCT. Again, in the static configura-

tion, the SP method is not preferred when compared to TCT, while the dynamic switching between the two configurations does not give any significant performance change.

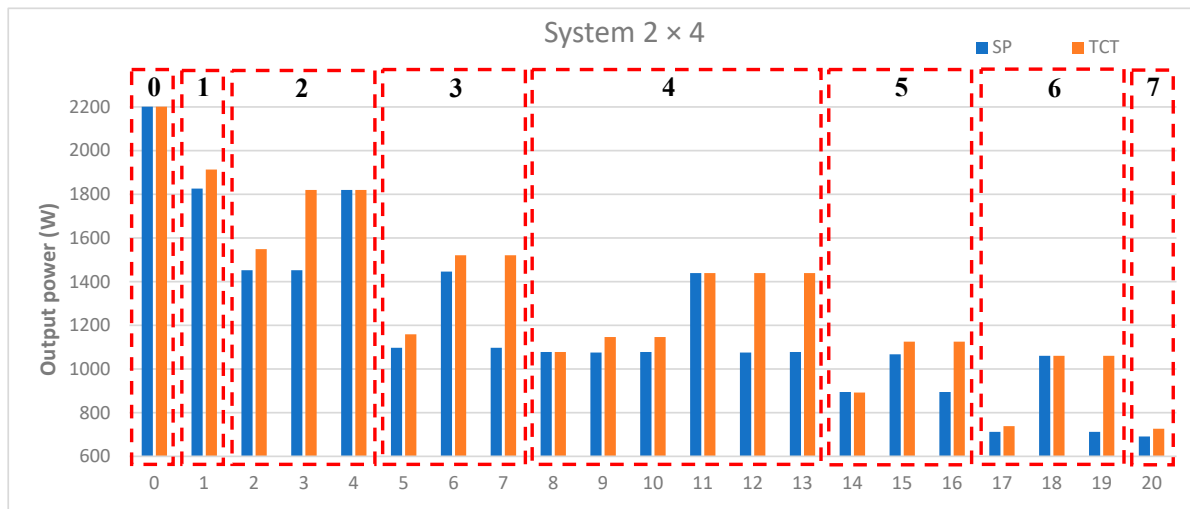


Figure 9. Bar chart of the output power for all 2×4 system cases.

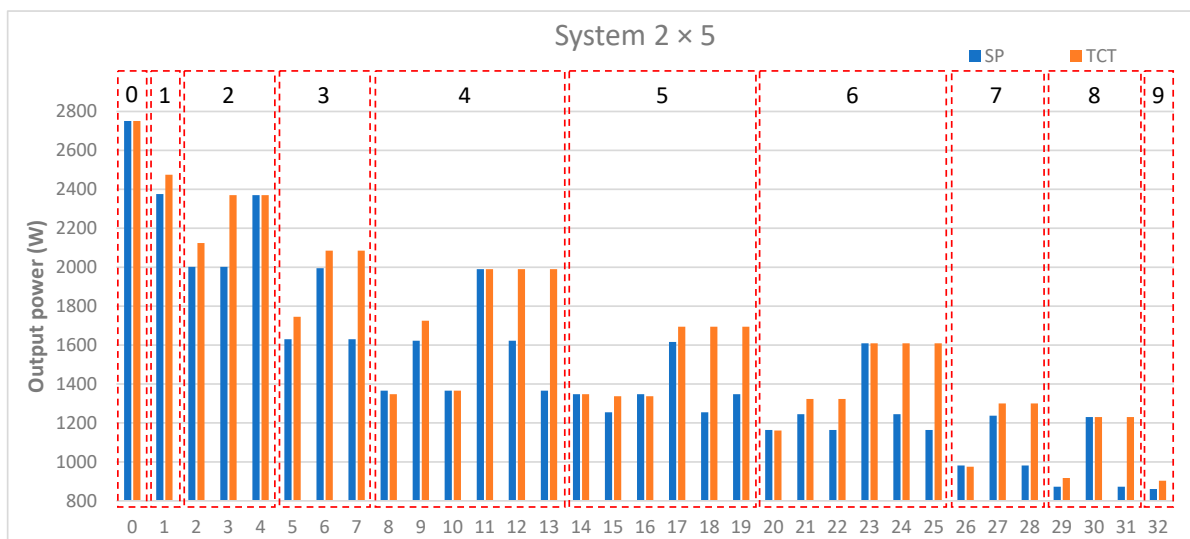


Figure 10. Bar chart of the output power for all 2×5 system cases.

Reconfigurable TCT can give an output power better than TCT. The performance is improved in seven states when using TCT-reconfiguration, with a noticeable percentage of power improvement. It can improve one case, in each group of two, three, seven, and eight shaded modules, with 10.38% in case 2, 16.31% in case 5, 25% in case 26, and 25.4% in case 29, respectively. The improvement is more significant in the states of four, five, and six shaded modules. In each of the three states, there are six possible cases. Half of them have the highest possible power, where reconfigurable TCT can improve the other half to give output power as the first half. The improvement ratio can be as large as 32.26% as in case 8.

Additionally, it is worth mentioning that the TCT introduces a higher V_{MPP} value, compared to that of SP, in a quarter of the possible cases, while it is almost equal in the rest of the cases. Consequently, the TCT-reconfiguration method ensures the highest possible V_{MPP} value in all cases.

From the I-V and P-V characteristic curves of the 32 cases that are shown in Figure A5, the best case for the TCT reconfiguration can be determined along with the location of the

global MPP. Moreover, a comparison between the partial pattern and the unshaded case may be conducted. The full simulated performance parameters are reported in Table A5.

7. Conclusions

The present study presents a performance investigation of small PV systems under all possible shading patterns. Small systems are defined as those consisting of 10 modules or fewer. There are five configurations that are most commonly used; two of which are symmetrical (2×2 and 3×3) and three are asymmetrical (2×3 , 2×4 , and 2×5). The main techniques of small static systems are SP and TCT.

All possible shading patterns, arising from a single shading level (300 W/m^2) under the two wiring techniques (SP and TCT), are studied. A new simplifying method is utilized to reduce the number of cases to be studied. The proposed method reduces the probable cases from 1862 to only 100 cases for the five systems. TCT configuration shows superiority in most cases, which makes TCT configuration the best static configuration for small PV systems. Some systems may follow the technique of dynamic switching between the (SP and TCT) according to the PS pattern to choose the best one. However, by applying this to small systems, it is notable that the amount of resultant improvement is slight or even has no value such as a 2×2 system. Thus, the extra complexity associated with dynamic switching does not compensate for the expected improvement.

The technique of TCT-reconfiguration (in which the shaded modules positions are re-arranged in the array according to the PS pattern by changing the electrical connections) is also tested to obtain the highest possible performance. Significant improvement is observed in a large number of cases in all small PV systems. This improvement occurs with the increase in the number of shaded units in half the system. The only drawback of this method is the need for many connections. However, due to the limited size of these systems, the required cable lengths are not long.

Hence, it is highly recommended to those who intend to develop their custom systems not to adopt dynamic switching configuration, but to implement TCT-reconfiguration. Furthermore, those who prefer to stick to static-configuration systems for their simplicity should follow the configurations of static TCT. Table 3 summarizes the number of cases in which TCT excelled in static configurations, in front of the number of cases that improved when transitioning to the dynamic switching between the SP and TCT configurations. The number of improved cases with TCT-reconfiguration techniques is also compared to the static TCT.

Table 3. All possible numbers of improved cases according to the configuration.

Configuration\System	2×2	3×3	2×3	2×4	2×5	
Static	TCT better	3	24	7	15	23
	SP better	2	4	1	1	3
	Equal	0	4	3	4	6
Dynamic better than static TCT by	0	4	1	1	3	
TCT-Reconfiguration better than static TCT by	1	14	3	7	13	
Total cases number	5	32	11	20	32	

Author Contributions: Conceptualization, M.A.M.Y., A.M.M. and Y.S.M.; methodology, A.M.M.; software, A.M.M.; validation, M.A.M.Y., Y.A.K. and Y.S.M.; formal analysis, M.A.M.Y.; investigation, A.M.M.; writing—original draft preparation, A.M.M.; writing—review and editing, A.M.M., Y.A.K. and M.A.M.Y.; supervision, M.A.M.Y. and Y.S.M.; project administration, M.A.M.Y.; funding acquisition, M.A.M.Y. All authors have read and agreed to the published version of the manuscript.

Funding: This work was funded by the Deanship of Scientific Research at Jouf University under grant No. (DSR-2021-02-03102).

Institutional Review Board Statement: Not applicable.

Informed Consent Statement: Not applicable.

Data Availability Statement: Not applicable.

Conflicts of Interest: The authors declare no conflict of interest.

Appendix A

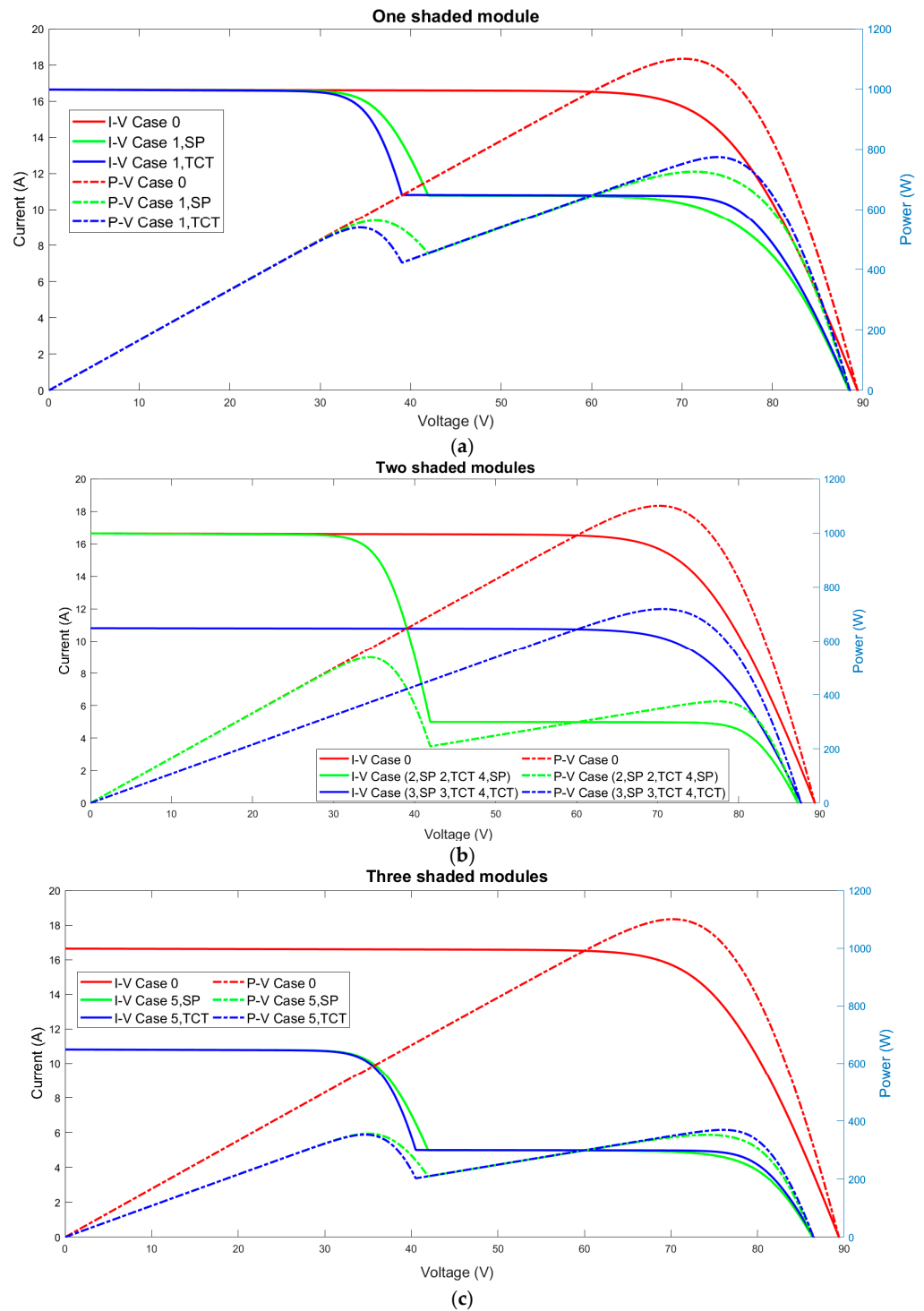


Figure A1. (I-V) and (P-V) characteristic curves of the PV 2 × 2 system under different numbers of shaded modules as follow: (a) One shaded module, (b) Two shaded modules, and (c) Three shaded modules.

Table A2. System 3 × 3 case studies and the resulted data.

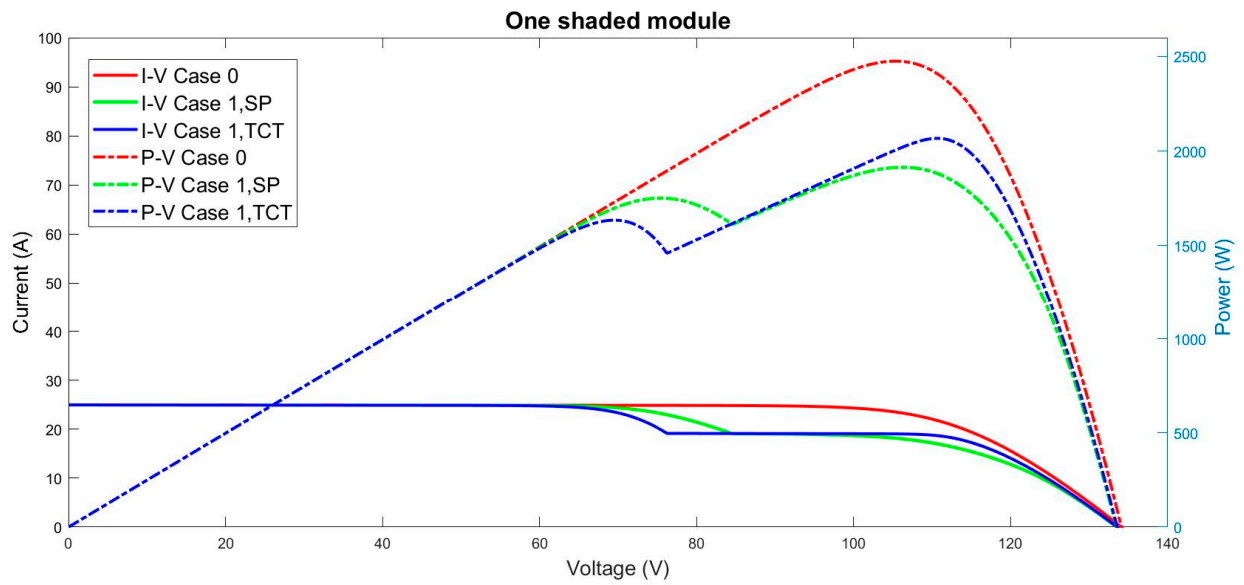
Case Number.	Number of Shaded Modules	Partial Shading Pattern	Series-Parallel										Total-Cross-Tied										
			V _{OC}	I _{SC}	V _{GMPP}	I _{GMPP}	P _{GMPP}	PL %	Efficiency %	Number of Local MPPs	V _{OC}	I _{SC}	V _{GMPP}	I _{GMPP}	P _{GMPP}	PL %	Efficiency %	Number of Local MPPs	K _{RT} %	K _{RT} %			
0	0	0 0 0				134.1	25	105.4	23.5	2476	0.00	14.18	1	134.1	25	105.4	23.5	2476	0.00	14.18	1	0.00	0.00
1	1	1 0 0	■			133.4	25	106.3	18	1914	22.70	10.96	2	133.5	25	110.7	18.7	2067	16.52	11.84	2	7.40	0.00
2	2	2 0 0	■	■		132.8	25	71.4	23.5	1674	32.39	9.59	2	132.9	25	69.6	23.5	1634	34.01	9.36	2	−2.45	17.39
3	2	1 1 0	■			132.9	25	106.1	18	1912	22.78	10.95	2	133	25	107.9	18.3	1978	20.11	11.33	2	3.34	0.00
4	1	1 1 0	■	■		132.8	25	71.4	23.5	1674	32.39	9.59	2	133	25	107.9	18.3	1978	20.11	11.33	2	15.37	0.00
5	3	3 0 0	■	■	■	132	25	96.6	23.5	1634	34.01	9.36	2	132	25	96.6	23.5	1634	34.01	9.36	2	0.00	14.23
6	2	2 1 0	■	■		132.1	25	108.2	12.5	1355	45.27	7.76	3	132.3	25	113.7	13	1481	40.19	8.48	3	8.51	22.26

Table A2. Cont.

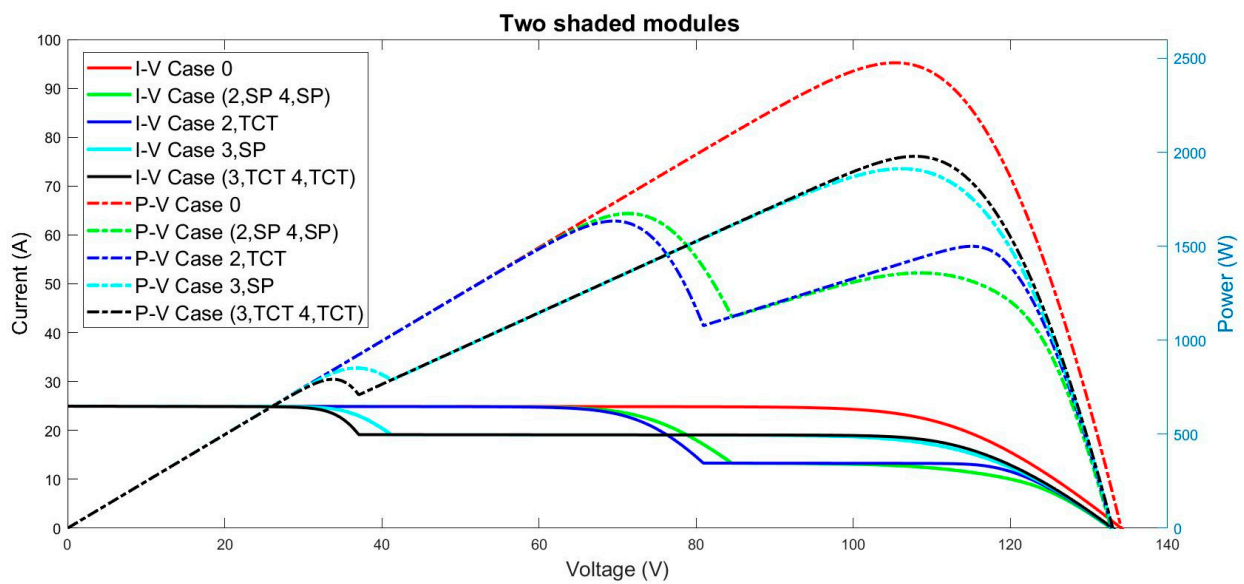
Case Number.	Number of Shaded Modules	Partial Shading Pattern	Series-Parallel									Total-Cross-Tied								
			V _{OC}	I _{SC}	V _{GMPP}	I _{GMPP}	P _{GMPP}	PL %	Efficiency %	Number of Local MPPs	V _{OC}	I _{SC}	V _{GMPP}	I _{GMPP}	P _{GMPP}	PL %	Efficiency %	Number of Local MPPs	K _{RT} %	K _{RT} %
14	2 2 0		131.3	25	70.1	18	1263	48.99	7.23	3	131.7	25	110.2	12.8	1410	43.05	8.07	2	10.43	3.56
		1 2 1																		
15	2 1 1		131.3	25	70.1	18	1263	48.99	7.23	3	131.8	19.2	112.3	13	1462	40.95	8.37	2	13.61	0.00
		1 1 2																		
16	1 2 1		131.6	25	107.9	12.5	1353	45.36	7.75	2	131.8	19.2	112.3	13	1462	40.95	8.37	2	7.46	0.00
		2 2 0																		
17	3 2 0		130.7	25	71.6	12.5	897	63.77	5.14	3	130.8	25	74.3	12.9	959.4	61.25	5.49	3	6.50	31.08
		2 2 1																		
18	2 2 1		131	19.2	107	12.6	1343	45.76	7.69	2	131.1	19.2	108.9	12.8	1392	43.78	7.97	2	3.52	0.00
		3 2 0																		
19	2 2 1		130.7	25	71.6	12.5	897	63.77	5.14	3	131.1	19.2	108.9	12.8	1392	43.78	7.97	2	35.56	0.00
		2 1 2																		
20	3 1 1		130.7	25	71.6	12.5	897	63.77	5.14	3	130.9	19.2	69.8	18	1257	49.23	7.20	2	28.64	9.70
		2 1 2																		

Table A2. Cont.

Case Number.	Number of Shaded Modules	Partial Shading Pattern	Series-Parallel									Total-Cross-Tied									K _{RT} %	K _{RT} %
			V _{OC}	I _{SC}	V _{GMPP}	I _{GMPP}	P _{GMPP}	PL %	Efficiency %	Number of Local MPPs	V _{OC}	I _{SC}	V _{GMPP}	I _{GMPP}	P _{GMPP}	PL %	Efficiency %	Number of Local MPPs				
28	2		130	19.1	71.7	12.5	896.7	63.78	5.13	3	130.5	13.3	106.3	12.6	1334	46.12	7.64	1	32.78	0.00		
	2																					
	2																					
		3 2 1																				
29	3		129.3	19.2	111.1	7.2	759.2	69.34	4.35	2	129.3	19.2	112.3	7.2	811.2	67.24	4.65	2	6.41	7.92		
	3																					
	1																					
		3 2 2																				
30	7	3	129.4	13.3	71.7	12.5	896.4	63.80	5.13	2	129.6	13.3	70.2	12.6	880.8	64.43	5.04	2	-1.77	0.00		
		2																				
		2																				
		3 3 1																				
31	3		129.3	19.2	111.1	7.2	759.2	69.34	4.35	2	129.6	13.3	70.2	12.6	880.8	64.43	5.04	2	13.81	0.00		
	2																					
	2																					
		3 2 2																				
32	8	3	128.6	13.3	109.4	7.1	778.8	68.55	4.46	2	128.7	13.3	111.1	7.2	802.1	67.61	4.59	2	2.90	0.00		
		3																				
		2																				
		3 3 2																				



(a)



(b)

Figure A2. Cont.

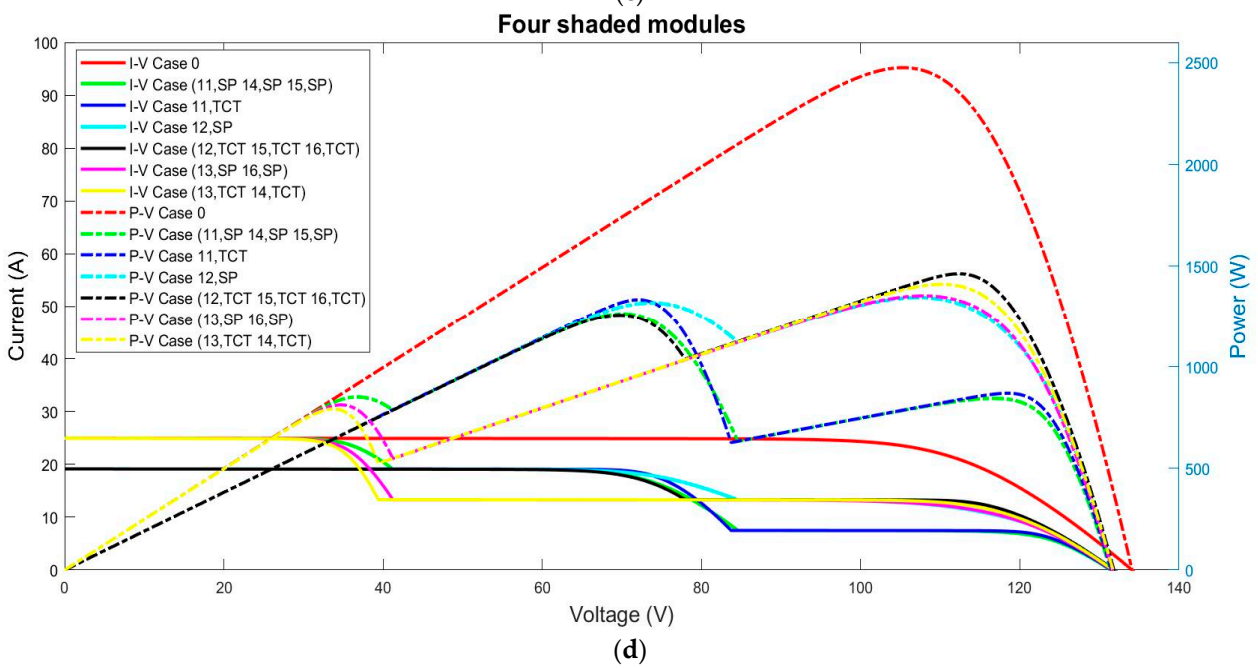
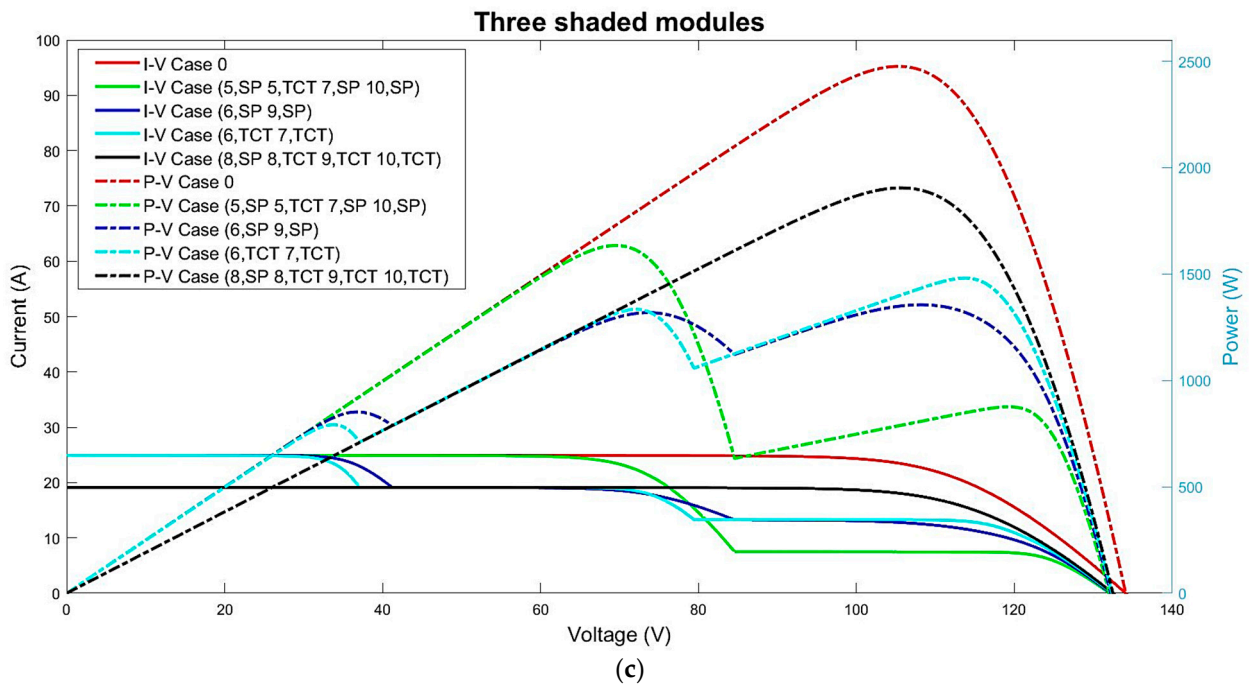


Figure A2. Cont.

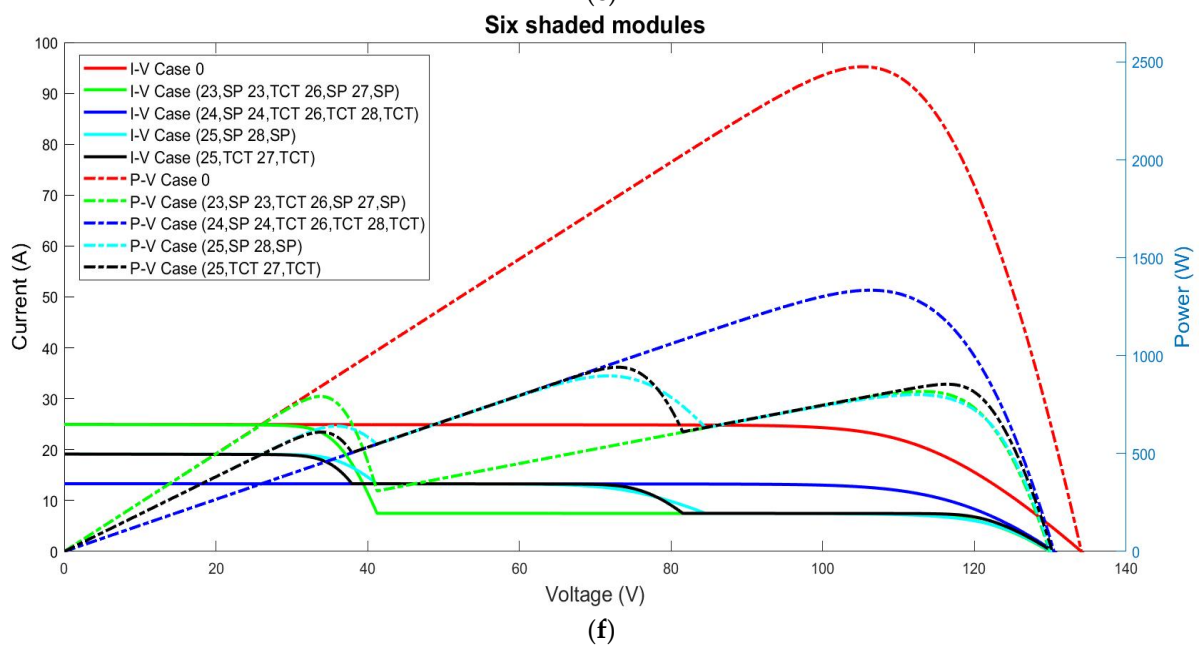
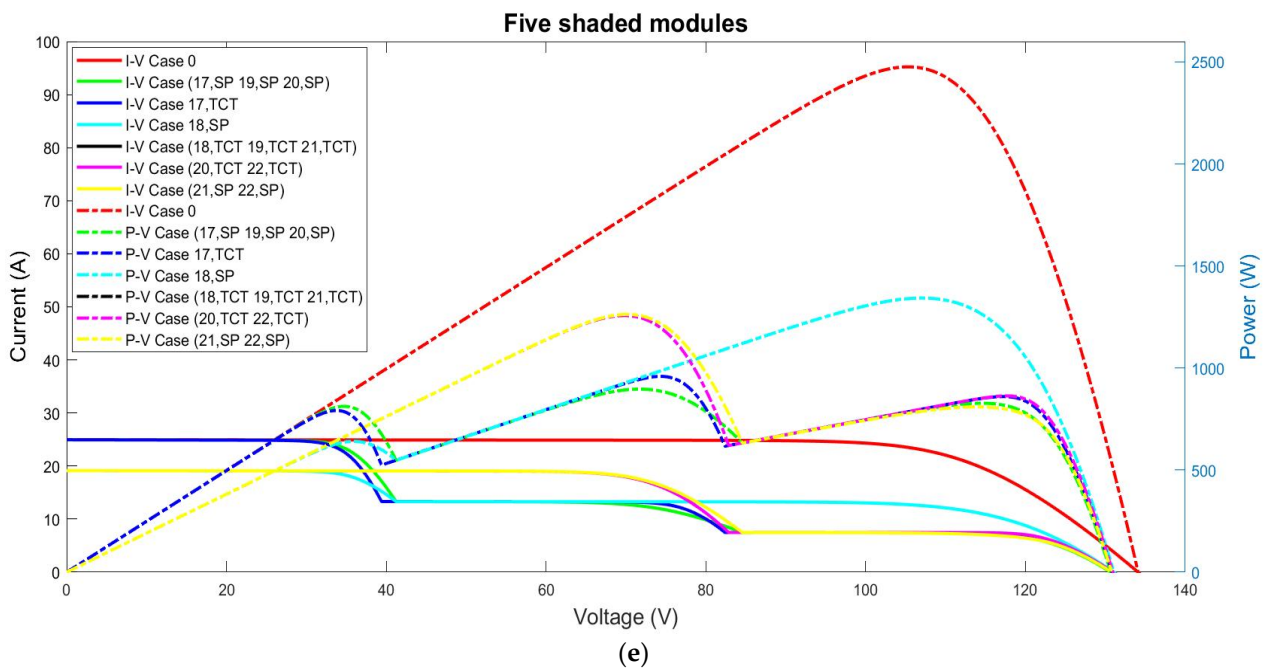


Figure A2. Cont.

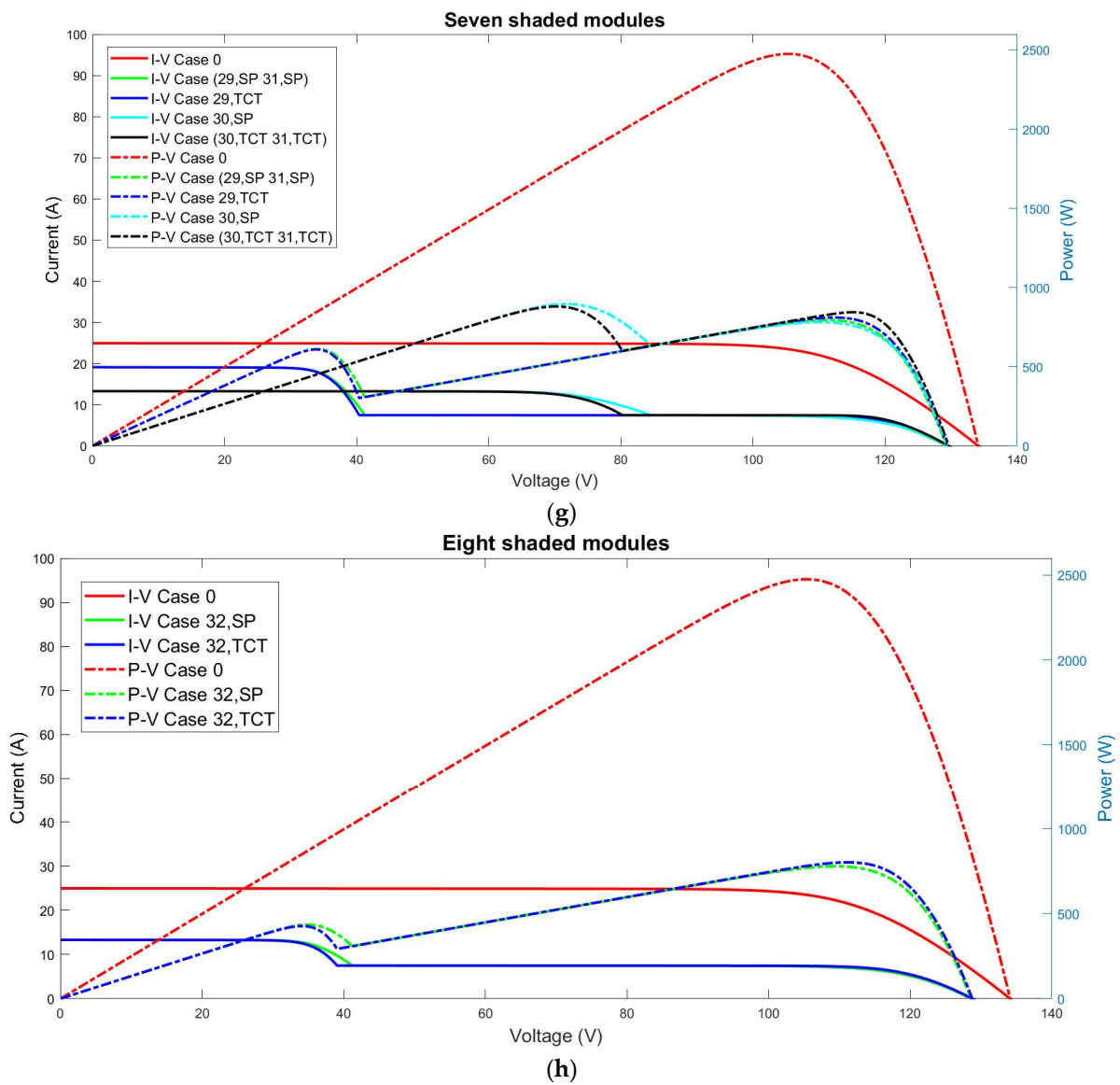


Figure A2. (I-V) and (P-V) characteristic curves of the PV 3×3 system under different numbers of shaded modules as follow: (a) One shaded module, (b) Two shaded modules, (c) Three shaded modules, (d) Four shaded modules, (e) Five shaded modules, (f) Six shaded modules, (g) Seven shaded modules, and (h) Eight shaded modules.

Table A3. System 2 × 3 case studies and the resulted data.

Case Number.	Number of Shaded Modules	Partial Shading Pattern	Series-Parallel										Total-Cross-Tied										
			V _{OC}	I _{sc}	V _{GMPP}	I _{GMPP}	P _{GMPP}	PL %	Efficiency %	Number of Local MPPs	V _{OC}	I _{sc}	V _{GMPP}	I _{GMPP}	P _{GMPP}	PL %	Efficiency %	Number of Local MPPs	K _{RT} %	K _{RT} %			
0	0	0	0	0	0	89.4	25	70.2	23.5	1651	0.00	14.18	1	89.4	25	70.2	23.5	1651	0.00	14.18	1	0.00	0.00
1	1	0	1	0	0	88.8	25	70.8	18	1276	22.71	10.96	2	88.8	25	72.8	18.5	1347	18.41	11.57	2	5.27	0.00
		1	0	0	88.1	25	72.2	12.5	904.5	45.22	7.77	2	88.8	25	75	12.9	968.5	41.34	8.32	2	6.61	23.74	
3	2	1	1	0	88.3	19.2	70.4	18	1270	23.08	10.91	1	88.3	19.2	70.4	18	1270	23.08	10.91	1	0.00	0.00	
		2	0	0	88.1	25	72.2	15.5	904.5	45.22	7.77	2	88.3	19.2	70.4	18	1270	23.08	10.91	1	28.78	0.00	
5	3	0	1	1	1	87.3	25	34.4	23.5	808.7	51.02	6.95	2	87.7	25	34.4	23.5	808.7	51.02	6.95	2	0.00	14.89
		1	2	0	87.6	19.2	71.5	12.5	896.3	45.71	7.70	2	87.6	19.2	73.7	12.9	950.2	42.45	8.16	2	5.67	0.00	
7	2	1	1	1	87.3	25	34.4	23.5	807.7	51.08	6.94	2	87.6	19.2	73.7	12.9	950.2	42.45	8.16	2	15.00	0.00	
		2	1	1	86.7	19.2	34.8	18	625.3	62.13	5.37	2	86.8	19.2	34.6	18	622.2	62.31	5.34	2	−0.50	30.06	

Table A3. Cont.

Case Number.	Number of Shaded Modules	Partial Shading Pattern	Series-Parallel									Total-Cross-Tied																
			V _{OC}	I _{SC}	V _{GMPP}	I _{GMPP}	P _{GMPP}	PL %	Efficiency %	Number of Local MPPs	V _{OC}	I _{SC}	V _{GMPP}	I _{GMPP}	P _{GMPP}	PL %	Efficiency %	Number of Local MPPs	K _T %	K _{RT} %								
9	4	2	[Shaded]				[Normal]				87	13.3	70.9	12.6	889.6	46.12	7.64	1	87	13.3	70.9	12.6	889.6	46.12	7.64	1	0.00	0.00
		2	2	0																								
10	4	2	[Shaded]				[Normal]				86.7	19.2	34.8	18	625.3	62.13	5.37	2	87	13.3	70.9	12.6	889.6	46.12	7.64	2	29.71	0.00
		2	1	1																								
11	5	3	[Shaded]				[Normal]				86	13.3	73.3	7.1	521	68.44	4.48	2	86.1	13.3	75.3	7.3	548.1	66.80	4.71	2	4.94	0.00
		2	2	1																								

Table A4. System 2 × 4 case studies and the resulted data.

Case Number.	Number of Shaded Modules	Partial Shading Pattern	Series-Parallel									Total-Cross-Tied																
			V _{OC}	I _{SC}	V _{GMPP}	I _{GMPP}	P _{GMPP}	PL %	Efficiency %	Number of Local MPPs	V _{OC}	I _{SC}	V _{GMPP}	I _{GMPP}	P _{GMPP}	PL %	Efficiency %	Number of Local MPPs	K _T %	K _{RT} %								
0	0	0	[Normal]				[Normal]				89.4	33.3	70.2	31.4	2201	0.00	14.18	1	89.4	33.3	70.2	31.4	2201	0.00	14.18	1	0.00	0.00
		0	0	0	0																							
1	1	1	[Shaded]				[Normal]				89	33.3	70.6	25.9	1826	17.04	11.76	2	89	33.3	72.9	26.5	1913	13.08	12.32	2	4.55	0.00
		0	1	0	0																							
2	0	2	[Shaded]				[Normal]				88.5	33.3	71.3	20.4	1452	34.03	9.35	2	88.5	33.3	73.9	21	1549	29.62	9.98	2	6.26	14.89
		1	1	0	0																							

Table A4. Cont.

Case Number.	Number of Shaded Modules	Partial Shading Pattern	Series-Parallel					Total-Cross-Tied																
			V _{OC}	I _{SC}	V _{GMPP}	I _{GMPP}	P _{GMPP}	PL %	Efficiency %	Number of Local MPPs	V _{OC}	I _{SC}	V _{GMPP}	I _{GMPP}	P _{GMPP}	PL %	Efficiency %	Number of Local MPPs	K _r %	K _{RT} %				
3	2	1																						
		1																						
			1	1	0	0	88.5	33.3	71.3	20.4	1452	34.03	9.35	2	88.6	27.5	70.4	25.9	1820	17.31	11.72	1	20.22	0.00
4	1	1																						
		1																						
			2	0	0	0	88.6	27.5	70.4	25.9	1820	17.31	11.72	1	88.6	27.5	70.4	25.9	1820	17.31	11.72	1	0.00	0.00
5	3	3																						
		0																						
			1	1	1	0	87.9	33.3	35.1	31.1	1097	50.16	7.07	2	88	33.3	75.5	15.3	1159	47.34	7.47	2	5.35	23.80
6	3	2																						
		1																						
			2	1	0	0	88	27.5	71	20.4	1446	34.30	9.32	2	88.2	27.5	72.7	20.9	1521	30.90	9.80	2	4.93	0.00
7	2	2																						
		1																						
			1	1	1	0	87.9	33.3	35.1	31.1	1097	50.16	7.07	2	88.2	27.5	72.7	20.9	1521	30.90	9.80	2	27.88	0.00
8	4	4																						
		0																						
			1	1	1	1	87.3	33.3	34.4	31.1	1078	51.02	6.94	2	87.3	33.3	34.4	31.1	1078	51.02	6.94	2	0.00	25.09
9	4	3																						
		1																						
			2	1	1	0	87.6	27.5	72.2	14.9	1075	51.16	6.93	2	87.6	27.5	74.7	15.3	1146	47.93	7.38	2	6.20	20.36
10	3	3																						
		1																						
			1	1	1	1	87.3	33.3	34.4	31.1	1078	51.02	6.94	2	87.6	27.5	74.7	15.3	1146	47.93	7.38	2	5.93	20.36
11	2	2																						
		2																						
			2	2	0	0	87.7	21.7	70.6	20.4	1439	34.62	9.27	1	87.7	21.7	70.6	20.4	1439	34.62	9.27	1	0.00	0.00

Table A4. Cont.

Case Number.	Number of Shaded Modules	Partial Shading Pattern	Series-Parallel							Total-Cross-Tied										
			V _{OC}	I _{SC}	V _{GMPP}	I _{GMPP}	P _{GMPP}	PL %	Efficiency %	Number of Local MPPs	V _{OC}	I _{SC}	V _{GMPP}	I _{GMPP}	P _{GMPP}	PL %	Efficiency %	Number of Local MPPs	K _r %	K _{RT} %
12	2		87.5	27.5	72.2	14.9	1075	51.16	6.93	2	87.7	21.7	70.6	20.4	1439	34.62	9.27	1	25.30	0.00
	2																			
13	2		87.3	33.3	34.4	31.1	1078	51.02	6.94	2	87.7	21.7	70.6	20.4	1439	34.62	9.27	1	25.09	0.00
	2																			
14	4		86.8	27.5	34.6	25.8	894.7	59.35	5.76	2	86.8	27.5	34.5	25.8	891.8	59.48	5.74	2	−0.33	20.73
	1																			
15	3		87	21.7	71.6	14.9	1067	51.52	6.87	2	87.1	21.7	73.5	15.3	1125	48.89	7.25	2	5.16	0.00
	2																			
16	3		86.8	27.5	34.6	25.8	894.7	59.35	5.76	2	87.1	21.7	73.5	15.3	1125	48.89	7.25	2	20.47	0.00
	2																			
17	4		86.3	21.7	35	20.3	712.2	67.64	4.59	2	86.5	21.7	76	9.7	738	66.47	4.75	2	3.50	30.38
	2																			
18	3		86.6	15.8	71	14.9	1060	51.84	6.83	1	86.6	15.8	71	14.9	1060	51.84	6.83	1	0.00	0.00
	3																			
19	3		86.3	21.7	35	20.3	712.2	67.64	4.59	2	86.6	15.8	71	14.9	1060	51.84	6.83	1	32.81	0.00
	3																			
20	4		85.5	15.8	72.9	9.5	690.8	68.61	4.45	2	85.9	15.8	74.9	9.7	726.1	67.01	4.68	2	4.86	0.00
	3																			

Table A5. Cont.

Case Number.	Number of Shaded Modules	Partial Shading Pattern	Series-Parallel					Total-Cross-Tied												
			V _{OC}	V _{SC} _{GMP}	I _{GMP}	P _{GMP}	PL %	Efficiency %	Number of Local MPPs	V _{OC}	I _{SC}	V _{GMP}	I _{GMP}	P _{GMP}	PL %	Efficiency %	Number of Local MPPs	K _T %	K _{RT} %	
9	3		87.9	35.8	71.4	22.7	1622	41.04	8.36	2	88	35.8	73.8	23.4	1725	37.30	8.89	2	5.97	13.32
	1																			
10	3		87.8	41.6	34.9	39.1	1366	50.35	7.04	2	87.8	41.6	34.9	39.1	1366	50.35	7.04	2	0.00	31.36
	1																			
11	2		88	30	70.5	28.2	1990	27.66	10.26	1	88	30	70.5	28.2	1990	27.66	10.26	1	0.00	0.00
	2																			
12	2		87.9	35.8	71.4	22.7	1622	41.04	8.36	2	88	30	70.5	28.2	1990	27.66	10.26	1	18.49	0.00
	2																			
13	2		87.8	41.6	34.9	39.1	1366	50.35	7.04	2	88	30	70.5	28.2	1990	27.66	10.26	1	31.36	0.00
	2																			
14	5		87.3	41.6	34.3	39.2	1348	51.00	6.95	1	87.3	41.6	34.3	39.2	1348	51.00	6.95	1	0.00	20.43
	0																			
15	4		87.4	35.8	72.8	17.2	1255	54.38	6.47	2	87.6	35.8	75.3	17.8	1337	51.40	6.89	2	6.13	21.07
	1																			
16	4		87.3	41.6	34.3	39.2	1348	51.00	6.95	1	87.6	35.8	75.3	17.8	1337	51.40	6.89	2	−0.82	21.07
	1																			
17	3		87.6	30	71.1	22.7	1616	41.26	8.33	2	87.7	30	72.6	23.3	1694	38.42	8.73	2	4.60	0.00
	2																			

Table A5. Cont.

Case Number.	Number of Shaded Modules	Partial Shading Pattern	Series-Parallel					Total-Cross-Tied												
			V _{OC}	V _{GMPP} _{SC}	I _{GMPP}	P _{GMPP}	PL %	Efficiency %	Number of Local MPPs	V _{OC}	I _{SC}	V _{GMPP}	I _{GMPP}	P _{GMPP}	PL %	Efficiency %	Number of Local MPPs	K _T %	K _{RT} %	
18	3		87.4	35.8	72.8	17.2	1255	54.38	6.47	2	87.7	30	72.6	23.3	1694	38.42	8.73	2	25.91	0.00
	2																			
		1 1 2 1 0																		
19	3		87.3	41.6	34.3	39.2	1348	51.00	6.95	1	87.7	30	72.6	23.3	1694	38.42	8.73	2	20.43	0.00
	2																			
		1 1 1 1 1																		
20	5		86.9	35.8	34.6	33.7	1164	57.69	6.00	2	87	35.8	34.5	33.7	1161	57.80	5.98	2	−0.26	27.84
	1																			
		2 1 1 1 1																		
21	4		87.1	30	72.2	17.3	1245	54.74	6.42	2	87.2	30	74.5	17.8	1323	51.91	6.82	2	5.90	17.78
	2																			
		2 2 1 1 0																		
22	4		86.9	35.8	34.6	33.7	1164	57.69	6.00	2	87.2	30	74.5	17.8	1323	51.91	6.82	2	12.02	17.78
	2																			
		1 1 1 2 1																		
23	3		87.3	24.1	70.7	22.8	1609	41.51	8.29	1	87.3	24.1	70.7	22.8	1609	41.51	8.29	1	0.00	0.00
	3																			
		2 2 2 0 0																		
24	3		87.1	30	72.2	17.3	1245	54.74	6.42	2	87.3	24.1	70.7	22.8	1609	41.51	8.29	1	22.62	0.00
	3																			
		1 2 2 1 0																		
25	3		86.9	35.8	34.6	33.7	1164	57.69	6.00	2	87.3	24.1	70.7	22.8	1609	41.51	8.29	1	27.66	0.00
	3																			
		1 1 2 1 1																		
26	5		86.5	30	34.8	28.2	981.3	64.33	5.06	2	86.6	30	34.6	28.2	975	64.56	5.02	2	−0.65	25.00
	2																			
		2 2 1 1 1																		

Table A5. Cont.

Case Number.	Number of Shaded Modules	Partial Shading Pattern	Series-Parallel							Total-Cross-Tied										
			V _{OC}	V _{SC} _{GMP}	I _{GMP}	P _{GMP}	PL %	Efficiency %	Number of Local MPPs	V _{OC}	I _{SC}	V _{GMP}	I _{GMP}	P _{GMP}	PL %	Efficiency %	Number of Local MPPs	K _r %	K _{rT} %	
27	4		86.7	24.1	71.6	17.3	1237	55.03	6.37	2	86.8	24.1	73.4	17.7	1300	52.74	6.70	2	4.85	0.00
	3																			
28	4		86.5	30	34.8	28.2	981.3	64.33	5.06	2	86.8	24.1	73.4	17.7	1300	52.74	6.70	2	24.52	0.00
	3																			
29	5		86.1	24.1	73.6	11.9	872.6	68.28	4.50	2	86.2	24.1	75.6	12.1	917.5	66.65	4.73	2	4.89	25.41
	3																			
30	4		86.4	18.3	71.2	17.3	1230	55.29	6.34	1	86.4	18.3	71.2	17.3	1230	55.29	6.34	1	0.00	0.00
	4																			
31	4		86.1	24.1	73.6	11.9	872.6	68.28	4.50	2	86.4	18.3	71.2	17.3	1230	55.29	6.34	1	29.06	0.00
	4																			
32	5		85.7	18.3	72.7	11.8	860.9	68.71	4.44	2	85.8	18.3	74.5	12.1	903.2	67.17	4.65	2	4.68	0.00
	4																			

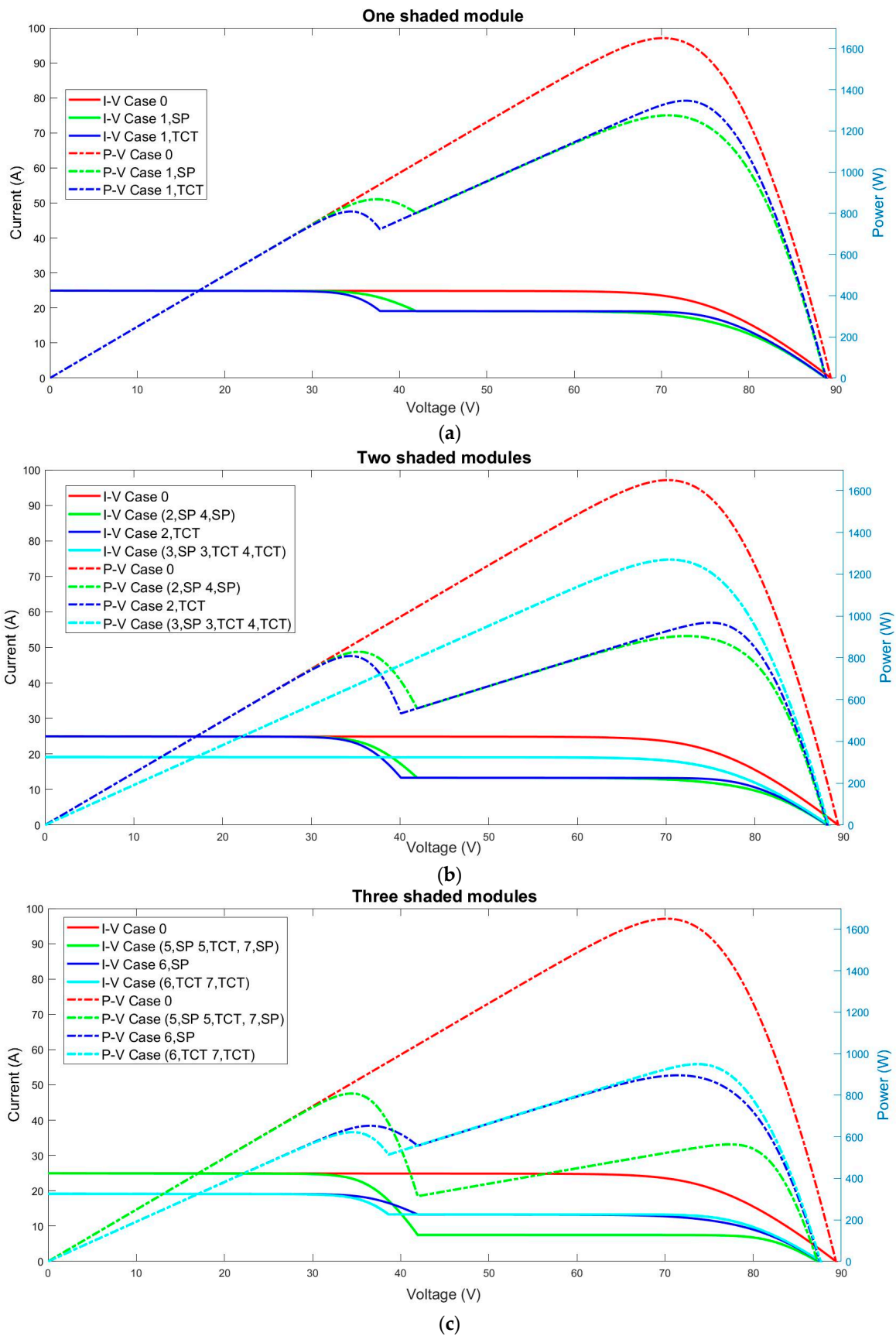


Figure A3. Cont.

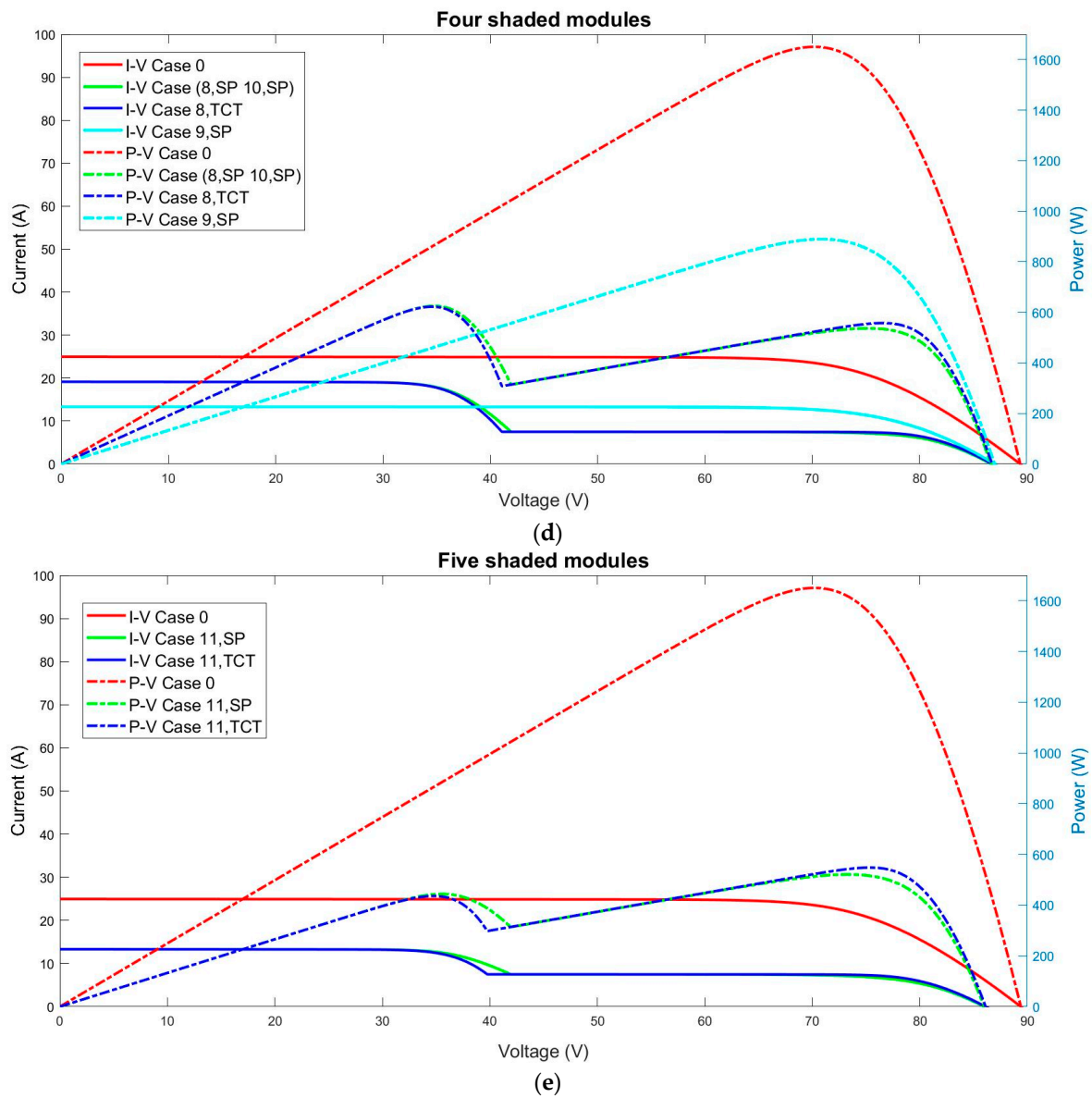


Figure A3. (I-V) and (P-V) Characteristic curves of the PV 2 × 3 system under different numbers of shaded modules as follow: (a) One shaded module, (b) Two shaded modules, (c) Three shaded modules, (d) Four shaded modules, and (e) Five shaded modules.

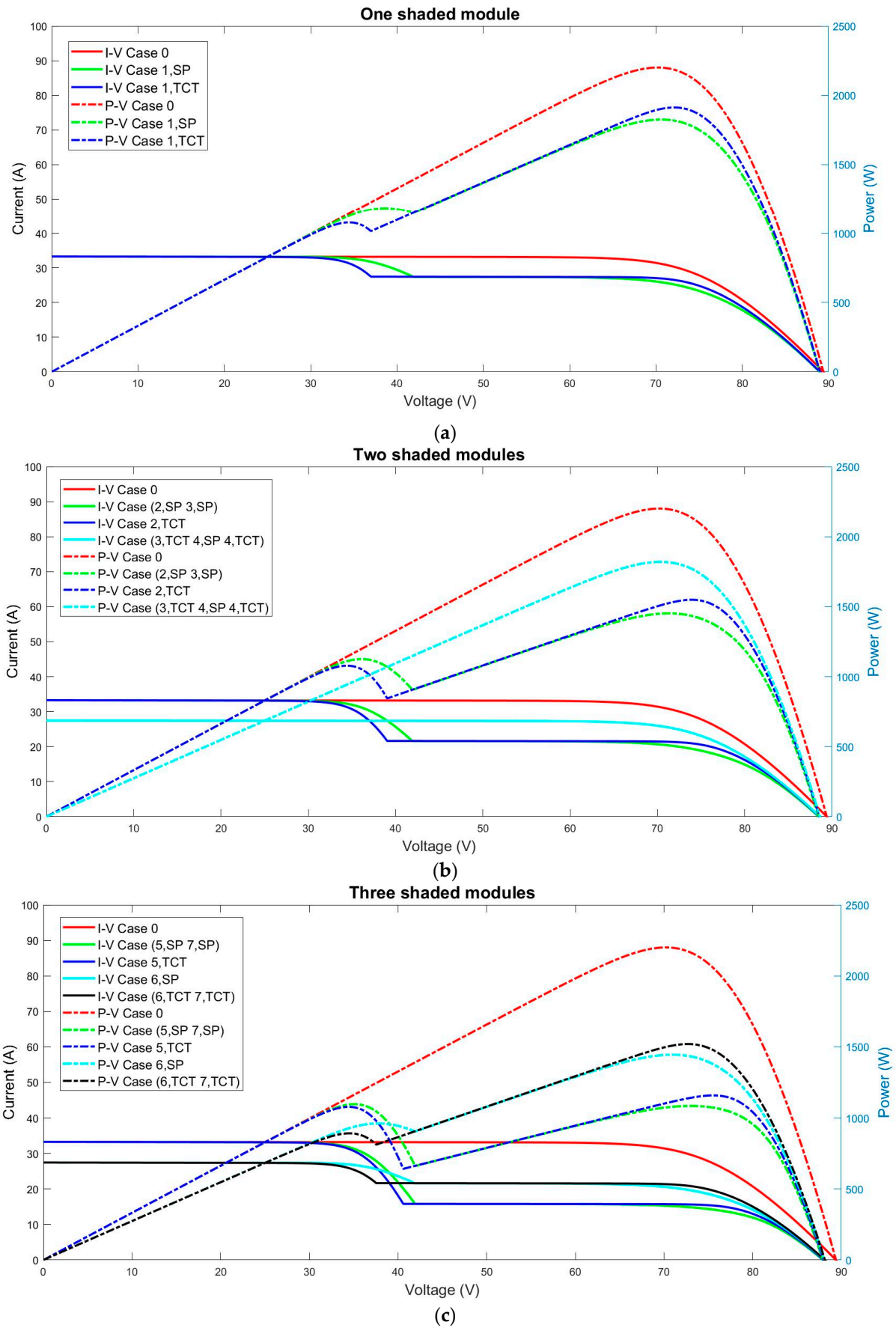


Figure A4. Cont.

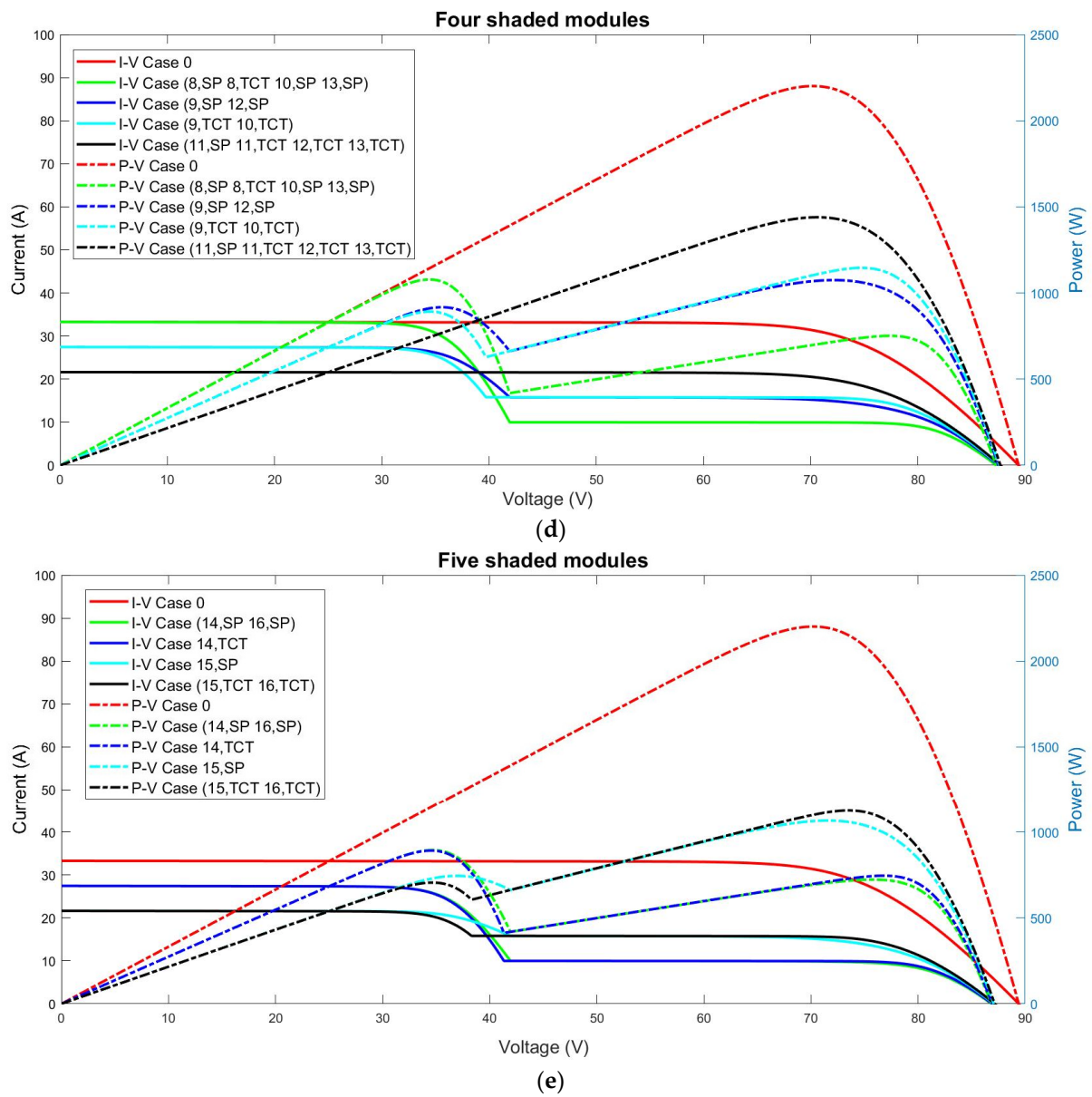


Figure A4. Cont.

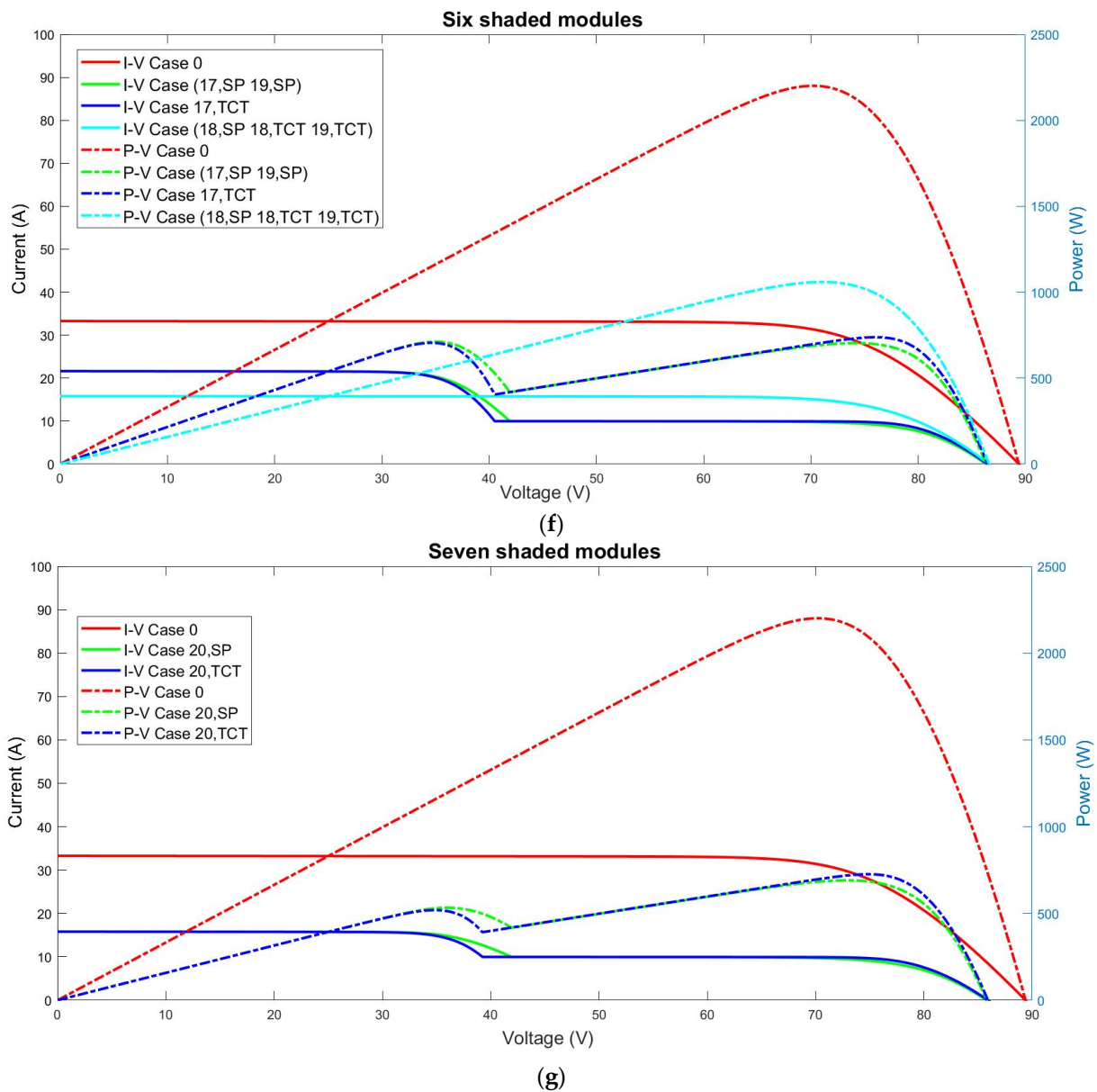


Figure A4. (I-V) and (P-V) Characteristic curves of the PV 2×4 system under different numbers of shaded modules as follow: (a) One shaded module, (b) Two shaded modules, (c) Three shaded modules, (d) Four shaded modules, (e) Five shaded modules, (f) Six shaded modules, and (g) Seven shaded modules.

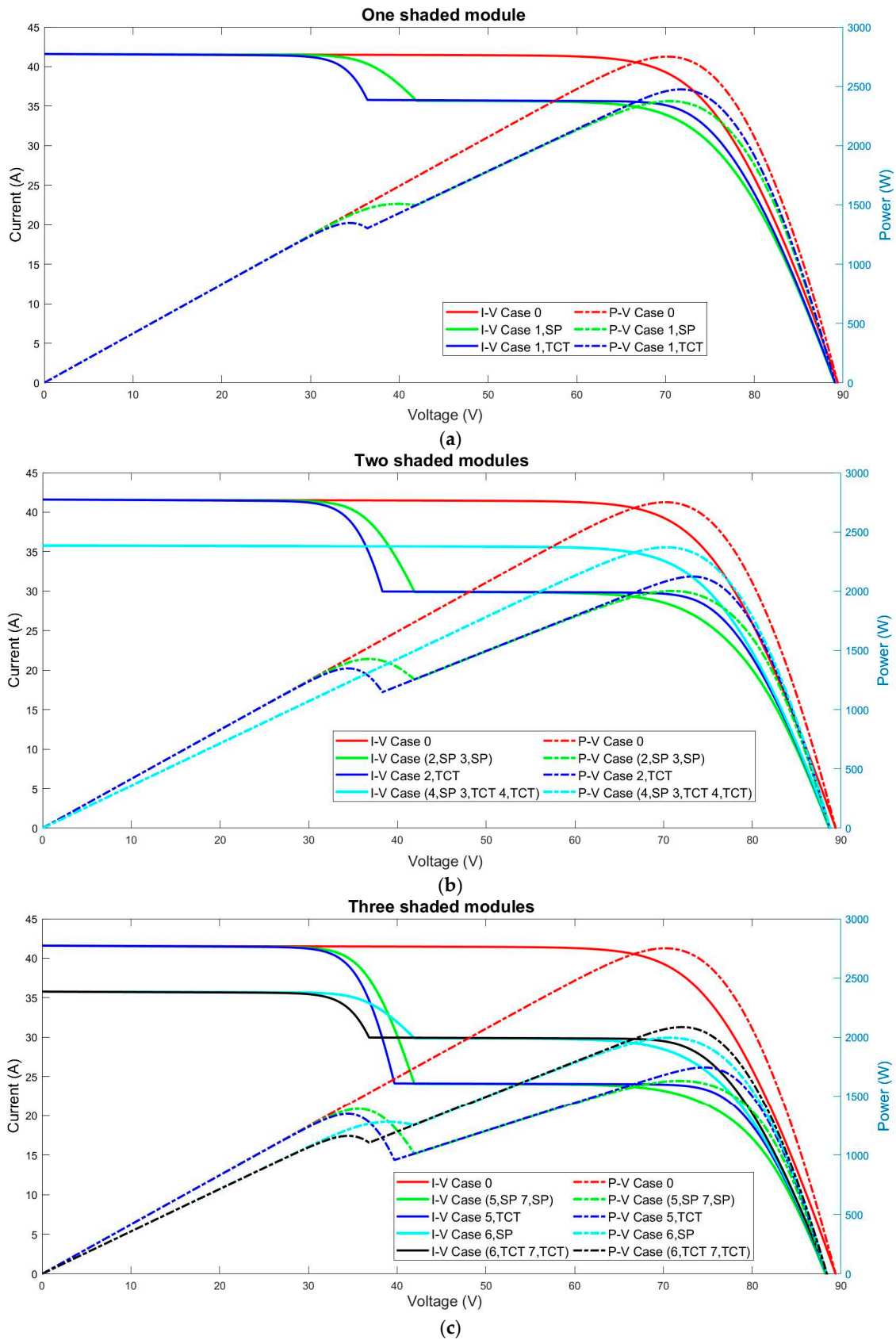
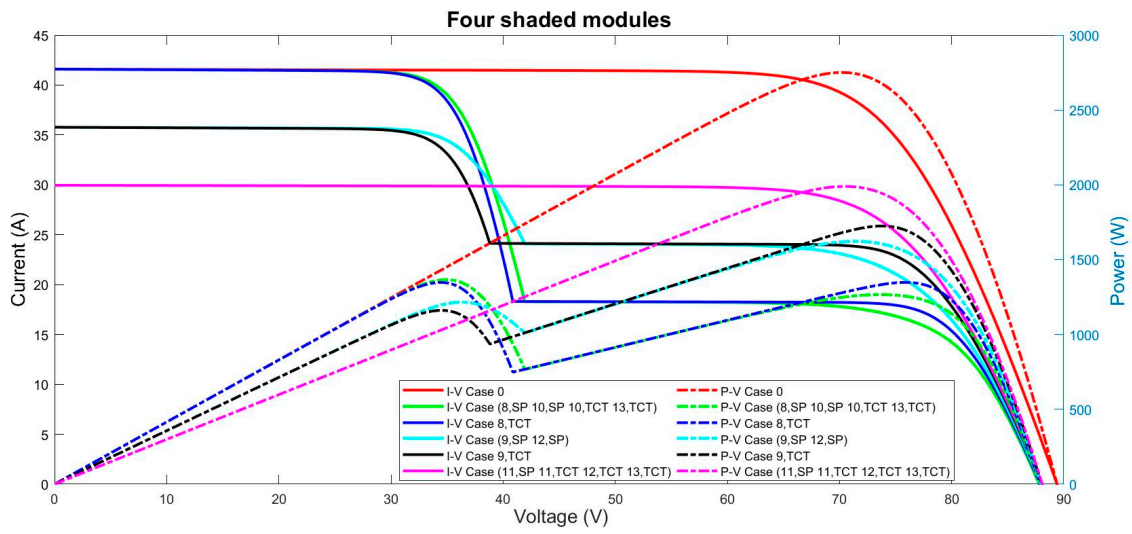
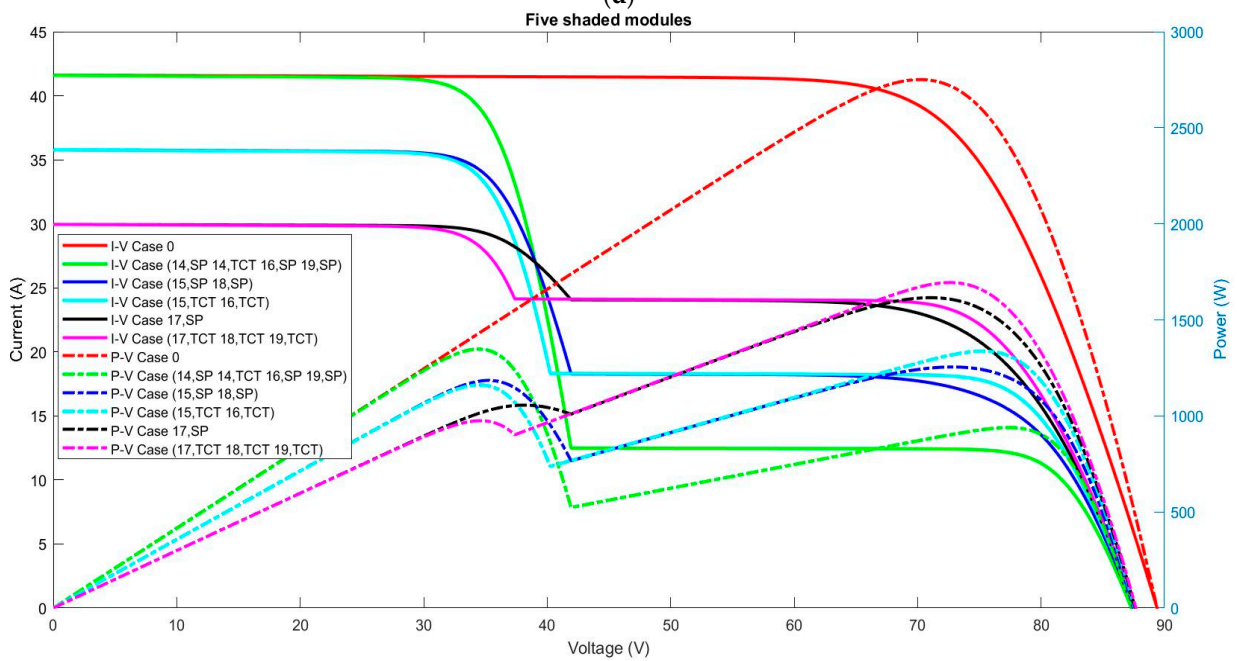


Figure A5. Cont.



(d)



(e)

Figure A5. Cont.

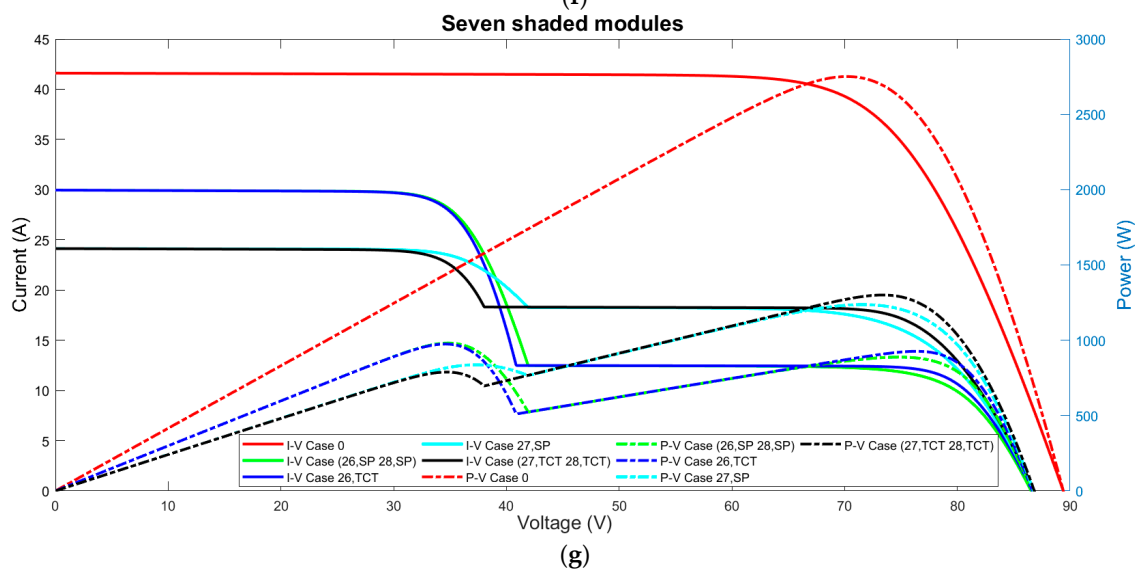
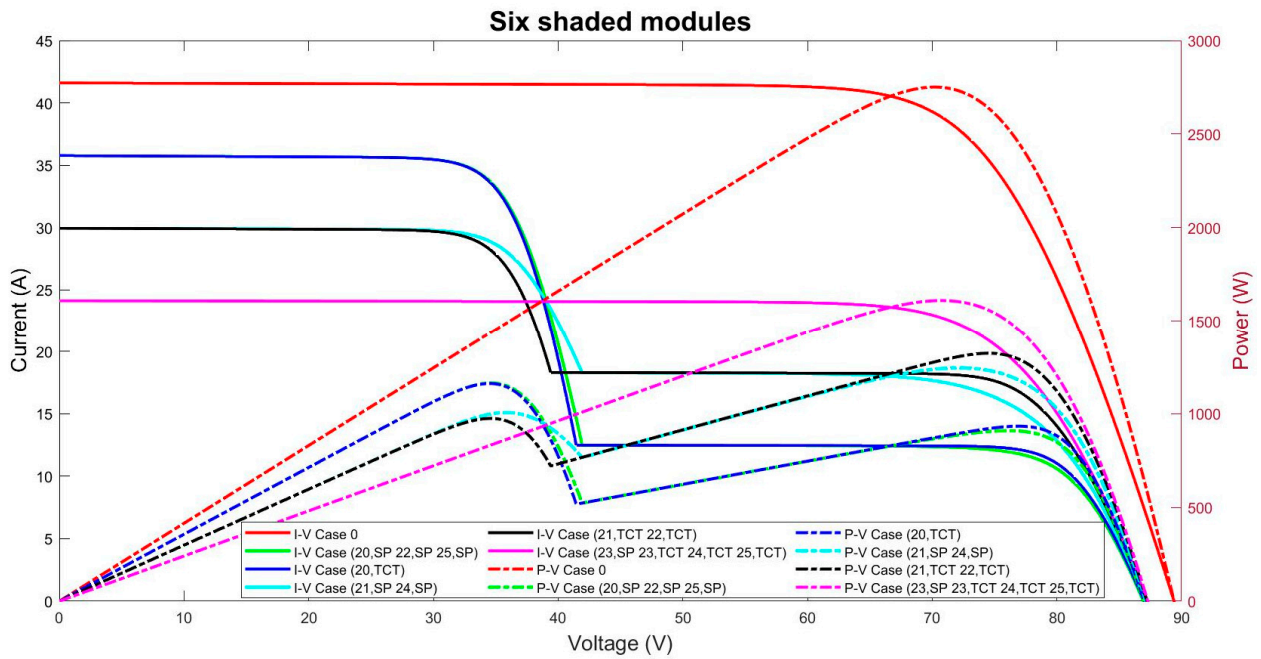


Figure A5. Cont.

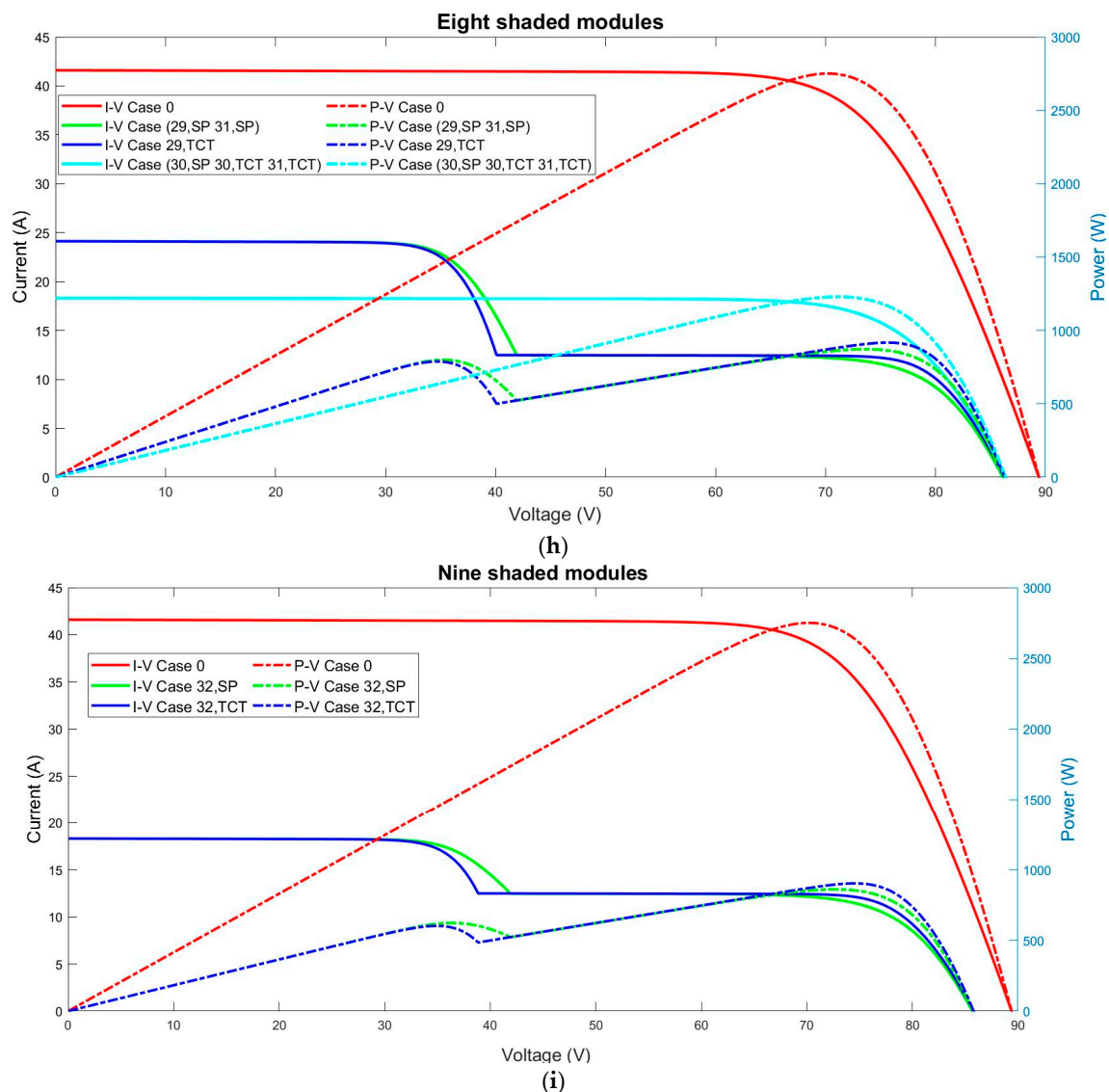


Figure A5. (I-V) and (P-V) characteristic curves of the PV 2×5 system under different numbers of shaded modules as follow: (a) One shaded module, (b) Two shaded modules, (c) Three shaded modules, (d) Four shaded modules, (e) Five shaded modules, (f) Six shaded modules, (g) Seven shaded modules, (h) Eight shaded modules, and (i) Nine shaded modules.

References

1. Bollipo, R.B.; Mikkili, S.; Bonthagorla, P.K. Critical review on PV MPPT techniques: Classical, intelligent and optimization. *IET Renew. Power Gener.* **2020**, *14*, 1433–1452. [CrossRef]
2. Subudhi, B.; Pradhan, R. A comparative study on maximum power point tracking techniques for photovoltaic power systems. *IEEE Trans. Sustain. Energy* **2013**, *4*, 89–98. [CrossRef]
3. Jiang, S.; Wan, C.; Chen, C.; Cao, E.; Song, Y. Distributed photovoltaic generation in the electricity market: Status, mode and strategy. *CSEE J. Power Energy Syst.* **2018**, *4*, 263–272. [CrossRef]
4. Wood, J. Renewable energy could power the world by 2050. Here's what that future might look like. *World Econ. Forum* **2020**. Available online: <https://www.weforum.org/agenda/2020/02/renewable-energy-future-carbon-emissions/> (accessed on 3 January 2022).
5. Reindl, K.; Palm, J. Installing PV: Barriers and enablers experienced by non-residential property owners. *Renew. Sustain. Energy Rev.* **2021**, *141*, 110829. [CrossRef]
6. Kılıç, U.; Kekezoğlu, B. A review of solar photovoltaic incentives and Policy: Selected countries and Turkey. *Ain Shams Eng. J.* **2022**, *13*, 101669. [CrossRef]
7. Almasri, R.A.; Alardhi, A.A.; Dilshad, S. Investigating the Impact of Integration the Saudi Code of Energy Conservation with the Solar PV Systems in Residential Buildings. *Sustainability* **2021**, *13*, 3384. [CrossRef]

8. Mokhtara, C.; Negrou, B.; Settou, N.; Bouferrouk, A.; Yao, Y. Optimal design of grid-connected rooftop PV systems: An overview and a new approach with application to educational buildings in arid climates. *Sustain. Energy Technol. Assess.* **2021**, *47*, 101468. [CrossRef]
9. Yousri, D.; Babu, T.S.; Mirjalili, S.; Rajasekar, N.; Elaziz, M.A. A Novel Objective Function with Artificial Ecosystem-Based Optimization for Relieving the Mismatching Power Loss of Large-Scale Photovoltaic Array. *Energy Convers. Manag.* **2020**, *225*, 113385. [CrossRef]
10. Shimizu, T.; Hirakata, M.; Kamezawa, T.; Watanabe, H. Generation control circuit for photovoltaic modules. *IEEE Trans. Power Electron.* **2001**, *16*, 293–300. [CrossRef]
11. Ali, A.; Almutairi, K.; Padmanaban, S.; Tirth, V.; Algarni, S. Investigation of MPPT techniques under uniform and non-uniform solar irradiation condition—A retrospection. *IEEE Access* **2020**, *8*, 127368–127392. [CrossRef]
12. Sahu, H.S.; Nayak, S.K.; Mishra, S. Maximizing the Power Generation of a Partially Shaded PV Array. *IEEE J. Emerg. Sel. Top. Power Electron.* **2016**, *4*, 626–637. [CrossRef]
13. Mohamed, A.M.A.; El-Sayed, A.; Mohamed, Y.S.; Ramadan, H.A. Enhancement of photovoltaic system performance based on different array topologies under partial shading conditions. *J. Adv. Eng. Trends* **2021**, *40*, 49–62. [CrossRef]
14. Raj, A.; Gupta, M. Numerical Simulation and Comparative Assessment of Improved Cuckoo Search and PSO based MPPT System for Solar Photovoltaic System Under Partial Shading Condition. *Turk. J. Comput. Math. Educ.* **2021**, *12*, 3842–3855. Available online: <https://turcomat.org/index.php/turkbilmat/article/view/7755> (accessed on 3 January 2022).
15. Abri, W.A.; Abri, R.A.; Yousef, H.; Al-Hinai, A. A Simple Method for Detecting Partial Shading in PV Systems. *Energies* **2021**, *14*, 4938. [CrossRef]
16. Chalh, A.; Hammoumi, A.E.; Motahhir, S.; Ghzizal, A.E.; Derouich, A.; Masud, M.; AlZain, M.A. Investigation of Partial Shading Scenarios on a Photovoltaic Array's Characteristics. *Electronics* **2022**, *11*, 96. [CrossRef]
17. Seritan, G.-C.; Enache, B.-A.; Adochiei, F.-C.; Argatu, F.C.; Christodoulou, C.; Vita, V.; Toma, A.R.; Gandescu, C.H.; Hathazi, F.-L. Performance Evaluation of Photovoltaic Panels Containing Cells with Different Bus Bars Configurations in Partial Shading Conditions. In *Revue Roumaine des Sciences Techniques—Electrotechnique et Energetique*; Romanian Academy, Publishing House of the Romanian Academy: Bucharest, Romania, 2020; Volume 65, pp. 67–70. ISSN 0035-4066. Available online: http://elth.pub.ro/~sepilus/REVUE/upload/77618212_GSeritan_RRST_1-2_2020_pp_67-70.pdf (accessed on 3 January 2022).
18. Sarniak, M.T. Modeling the Functioning of the Half-Cells Photovoltaic Module under Partial Shading in the Matlab Package. *Appl. Sci.* **2020**, *10*, 2575. [CrossRef]
19. Hanifi, H.; Schneider, J.; Bagdahn, J. Reduced Shading Effect on Half-Cell Modules—Measurement and Simulation. In Proceedings of the 31st European Photovoltaic Solar Energy Conference and Exhibition, Hamburg, Germany, 14–18 September 2015; pp. 2529–2533, ISBN 3-936338-39-6. [CrossRef]
20. Nazer, M.N.R.; Noorwali, A.; Tajuddin, M.F.N.; Khan, M.Z.; Tazally, M.A.I.A.; Ahmed, J.; Ghazali, N.H.; Chakraborty, C.; Kumar, N.M. Scenario-Based Investigation on the Effect of Partial Shading Condition Patterns for Different Static Solar Photovoltaic Array Configurations. *IEEE Access* **2021**, *9*, 116050–116072. [CrossRef]
21. Madhu, G.M.; Vyjayanthi, C.; Modi, C.N. Investigation on Effect of Irradiance Change in Maximum Power Extraction From PV Array Interconnection Schemes During Partial Shading Conditions. *IEEE Access* **2021**, *9*, 96995–97009. [CrossRef]
22. Bonthagorla, P.K.; Mikkili, S. Performance investigation of hybrid and conventional PV array configurations for grid-connected/standalone PV systems. *CSEE J. Power Energy Syst.* **2020**, *1*–16. [CrossRef]
23. Moballegh, S.; Jiang, J. Modeling, prediction, and experimental validations of power peaks of PV arrays under partial shading conditions. *IEEE Trans. Sustain. Energy* **2014**, *5*, 293–300. [CrossRef]
24. Elyaqouti, M.; Izbaim, D.; Bouhouch, L. Study of the Energy Performance of Different PV Arrays Configurations Under Partial Shading. *E3S Web Conf.* **2021**, *229*, 01044. [CrossRef]
25. Muhammad, A.; Babu, T.S.; Ramachandaramurthy, V.K.; Yousri, D.; Ekanayake, J.B. Static and dynamic reconfiguration approaches for mitigation of partial shading influence in photovoltaic arrays. *Sustain. Energy Technol. Assess.* **2020**, *40*, 100738. [CrossRef]
26. Mishra, N.; Yadav, A.S.; Pachauri, R.; Chauhan, Y.K.; Yadav, V.K. Performance enhancement of PV system using proposed array topologies under various shadow patterns. *Sol. Energy* **2017**, *157*, 641–656. [CrossRef]
27. Malathy, S.; Ramaprabha, R. Reconfiguration strategies to extract maximum power from photovoltaic array under partially shaded conditions. *Renew. Sustain. Energy Rev.* **2018**, *81*, 2922–2934. [CrossRef]
28. Bonthagorla, P.K.; Mikkili, S. A novel fixed PV array configuration for harvesting maximum power from shaded modules by reducing the number of cross-ties. *IEEE J. Emerg. Sel. Top. Power Electron.* **2021**, *9*, 2109–2121. [CrossRef]
29. Krishna, G.S.; Moger, T. Reconfiguration strategies for reducing partial shading effects in photovoltaic arrays: State of the art. *Sol. Energy* **2019**, *182*, 429–452. [CrossRef]
30. Pachauri, R.K.; Mahela, O.P.; Sharma, A.; Bai, J.; Chauhan, Y.K.; Khan, B.; Alhelou, H.H. Impact of partial shading on various PV array configurations and different modeling approaches: A comprehensive review. *IEEE Access* **2020**, *8*, 181375–181403. [CrossRef]
31. Venkateswari, R.; Rajasekar, N. Power enhancement of PV system via physical array reconfiguration based Lo Shu technique. *Energy Convers. Manag.* **2020**, *215*, 112885. [CrossRef]

32. Anjum, S.; Mukherjee, V.; Mehta, G. Hyper SuDoKu-Based Solar Photovoltaic Array Reconfiguration for Maximum Power Enhancement Under Partial Shading Conditions. *J. Energy Resour. Technol.* **2022**, *144*, 031302. [[CrossRef](#)]
33. Yang, B.; Shao, R.; Zhang, M.; Ye, H.; Liu, B.; Bao, T.; Wang, J.; Shu, H.; Ren, Y.; Ye, H. Socio-inspired democratic political algorithm for optimal PV array reconfiguration to mitigate partial shading. *Sustain. Energy Technol. Assess.* **2021**, *48*, 101627. [[CrossRef](#)]
34. Yousri, D.; Babu, T.S.; Beshr, E.; Eteiba, M.B.; Allam, D. A robust strategy based on marine predators' algorithm for large scale photovoltaic array reconfiguration to mitigate the partial shading effect on the performance of PV system. *IEEE Access* **2020**, *8*, 112407–112426. [[CrossRef](#)]
35. Zsiborács, H.; Zentkó, L.; Pintér, G.; Vincze, A.; Baranyai, N.H. Assessing shading losses of photovoltaic power plants based on string data. *Energy Rep.* **2021**, *7*, 3400–3409. [[CrossRef](#)]
36. Karmakar, B.K.; Karmakar, G. A Current Supported PV Array Reconfiguration Technique to Mitigate Partial Shading. *IEEE Trans. Sustain. Energy* **2021**, *12*, 1449–1460. [[CrossRef](#)]
37. Srinivasan, A.; Devakirubakaran, S.; Sundaram, B.M.; Balachandran, P.K.; Cherukuri, S.K.; Winston, D.P.; Babu, T.S.; Alhelou, H.H. L-Shape Propagated Array Configuration with Dynamic Reconfiguration Algorithm for Enhancing Energy Conversion Rate of Partial Shaded Photovoltaic Systems. *IEEE Access* **2021**, *9*, 97661–97674. [[CrossRef](#)]
38. Pachauri, R.K.; Kansal, I.; Babu, T.S.; Alhelou, H.H. Power Losses Reduction of Solar PV Systems Under Partial Shading Conditions Using Re-Allocation of PV Module-Fixed Electrical Connections. *IEEE Access* **2021**, *9*, 94789–94812. [[CrossRef](#)]
39. MANUALZZ the Universal Manuals Library, STP275_270_24Vd1. Available online: https://manualzz.com/doc/10607158/stp275_270_24vd1 (accessed on 3 January 2022).